

1-1-1995

## Experimental determination of pressures and velocities in plant xylem

Anand Kanjerla  
*University of Nevada, Las Vegas*

Follow this and additional works at: <https://digitalscholarship.unlv.edu/rtds>

---

### Repository Citation

Kanjerla, Anand, "Experimental determination of pressures and velocities in plant xylem" (1995). *UNLV Retrospective Theses & Dissertations*. 458.  
<http://dx.doi.org/10.25669/xquu-7lym>

This Thesis is protected by copyright and/or related rights. It has been brought to you by Digital Scholarship@UNLV with permission from the rights-holder(s). You are free to use this Thesis in any way that is permitted by the copyright and related rights legislation that applies to your use. For other uses you need to obtain permission from the rights-holder(s) directly, unless additional rights are indicated by a Creative Commons license in the record and/or on the work itself.

This Thesis has been accepted for inclusion in UNLV Retrospective Theses & Dissertations by an authorized administrator of Digital Scholarship@UNLV. For more information, please contact [digitalscholarship@unlv.edu](mailto:digitalscholarship@unlv.edu).

## INFORMATION TO USERS

This manuscript has been reproduced from the microfilm master. UMI films the text directly from the original or copy submitted. Thus, some thesis and dissertation copies are in typewriter face, while others may be from any type of computer printer.

**The quality of this reproduction is dependent upon the quality of the copy submitted.** Broken or indistinct print, colored or poor quality illustrations and photographs, print bleedthrough, substandard margins, and improper alignment can adversely affect reproduction.

In the unlikely event that the author did not send UMI a complete manuscript and there are missing pages, these will be noted. Also, if unauthorized copyright material had to be removed, a note will indicate the deletion.

Oversize materials (e.g., maps, drawings, charts) are reproduced by sectioning the original, beginning at the upper left-hand corner and continuing from left to right in equal sections with small overlaps. Each original is also photographed in one exposure and is included in reduced form at the back of the book.

Photographs included in the original manuscript have been reproduced xerographically in this copy. Higher quality 6" x 9" black and white photographic prints are available for any photographs or illustrations appearing in this copy for an additional charge. Contact UMI directly to order.

# UMI

A Bell & Howell Information Company  
300 North Zeeb Road, Ann Arbor, MI 48106-1346 USA  
313/761-4700 800/521-0600



**Experimental Determination of Pressures and Velocities  
in Plant Xylem**

by

**Anand Kanjerla**

A thesis submitted in partial fulfillment  
of the requirements of the degree of

Master of Science  
in  
Civil and Environmental Engineering

Department of Civil and Environmental Engineering  
University of Nevada, Las Vegas  
May 1995

UMI Number: 1374887

---

UMI Microform 1374887

Copyright 1995, by UMI Company. All rights reserved.

This microform edition is protected against unauthorized  
copying under Title 17, United States Code.

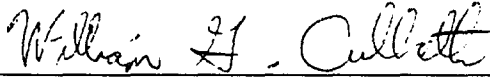
---

UMI

300 North Zeeb Road  
Ann Arbor, MI 48103

---

The thesis of Kanjerla Anand for the degree of Master of Science in Civil and Environmental Engineering is approved.



---

Chairperson, Professor William Culbreth, Ph.D



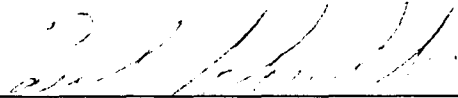
---

Examining Committee Member, Professor James Cardle, Ph.D



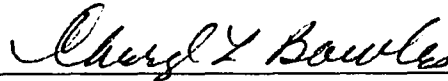
---

Examining Committee Member, Professor David James, Ph.D



---

Examining Committee Member, Professor Paul Schulte, Ph.D



---

Graduate Dean, Professor Cheryl L. Bowles, Ed.D

University of Nevada, Las Vegas  
May 1995

## ABSTRACT

This study reports on the experimental modeling of fluid flow in plant xylem. Three experiments were conducted to determine pressures and velocities in the conducting vessels of the xylem portion of a plant using corn syrup as the working fluid and Plexiglas tubing as the test section. The first experiment was performed using a straight duct to model the flow in a xylem vessel without any obstructions. The second experiment was performed using a 5-pore perforation plate as an obstruction in a straight duct. This perforation plate was kept at an angle of 23 degrees relative to the vessel axis to match the fluid flow through a perforation plate found in the plant species *Liriodendron tulipifera*. In the third experiment, a 20-pore perforation plate was used to match the vessels of *Liquidambar styraciflua*. This plate was placed at an angle of 12.7 degrees. To verify the flow behavior, the experimental results were compared with a numerical simulation using NEKTON, a computational fluid dynamics package. Experimental results and the numerical results agreed with each other. In the experiments involving the 20-pore perforation plate, the average loss coefficient was 86.300 over the range  $0.2 < Re_D < 0.5$ . The results of this work also consisted of plots of streamlines, velocity distributions, and pressure within the xylem.

## ACKNOWLEDGMENTS

I would like to express my gratitude to Dr. William Culbreth for his contribution rendered towards my thesis. But for his ideas and guidance at each step, this thesis could not have been possible.

I am deeply indebted to Dr. Paul Schulte of Biology Department for providing financial support and offering suggestions during various stages of this thesis.

I would also like to thank Dr. Samaan Ladkany, Professor of Civil and Environmental Engineering for offering me financial support in summer 1993. I sincerely thank Dr. James Cardle of Civil and Environmental Engineering for his suggestions and comments during my association with him as a teaching assistant. I am grateful to Dr. David James of Civil and Environmental Engineering for accepting to be on my committee, in spite of his busy schedule.

My sincere thanks go to Cray Research, Inc. for providing financial assistance under a research grant to support my work. Finally, I would like to thank my friends, Mr. Vasanth Rajagopalan, Mr. Rajkumar Rajagopalan and Dr. James Ventresca for their help during the course of this thesis. I acknowledge with gratitude, the help and support my parents and my brothers offered, during the course of my thesis. Last, but not least, I would like to thank the Department of Civil and Environmental Engineering for supporting me financially during the course of my studies.

## Table of Contents

|  |      |
|--|------|
| ABSTRACT.....  | iii  |
| ACKNOWLEDGMENTS .....  | iv   |
| NOMENCLATURE.....  | viii |
| CHAPTER 1 - INTRODUCTION .....                                     | 1    |
| 1.1 Overview .....   | 1    |
| CHAPTER 2 - REVIEW OF PAST WORK .....                              | 4    |
| 2.1 Literature Review .....  | 4    |
| CHAPTER 3 - THEORETICAL DESCRIPTION .....                          | 8    |
| 3.1 Stokes Flow.....   | 8    |
| 3.2 Velocity Distribution Through the Cross-Section of a Pipe..... | 10   |
| 3.3 Hagen-Poiseuille Flow .....                                    | 12   |
| 3.3.1 Derivation of Hagen-Poiseuille Equation.....                 | 12   |
| 3.4 Minor Losses .....   | 16   |
| CHAPTER 4 - EXPERIMENTAL SETUP AND PROCEDURE.....                  | 19   |
| 4.1 Overview.....  | 19   |
| 4.2 Experimental Setup .....                                       | 19   |
| 4.2.1 Working Fluid .....  | 20   |
| 4.2.2 Description of the Experimental Setup.....                   | 20   |
| 4.2.3 Instrumentation .....  | 23   |
| 4.3 Experimental Procedure .....                                   | 23   |
| 4.4 Uncertainty Analysis .....                                     | 26   |
| CHAPTER 5 - EXPERIMENTAL RESULTS.....                              | 31   |
| 5.1 Experimental Results - Straight Duct .....                     | 31   |
| 5.2 Experimental Results 5-Pore Perforation Plate.....             | 32   |
| 5.3 Experimental Results 20-Pore Perforation Plate .....           | 32   |
| CHAPTER 6 - NUMERICAL RESULTS.....                                 | 36   |

|  |    |
|--|----|
| CHAPTER 7 - CONCLUSIONS AND RECOMMENDATIONS .....                  | 53 |
| APPENDIX I - COMPUTER PROGRAMS .....                               | 56 |
| A: Program Cor1 .....  | 56 |
| B: Program Cor2 .....  | 58 |
| C: Program Cor3 .....  | 59 |
| D: Program Cor4 .....  | 61 |
| E: Program Cor5 .....  | 63 |
| APPENDIX II - TABULATED RESULTS .....                              | 67 |
| II.1 Data for the Plot of Friction Factor vs Reynolds Number ..... | 67 |
| II.2 Data for 5-Pore Perforation Plate .....                       | 68 |
| II.3 Data for the Plot of Loss Coefficient vs Reynolds Number..... | 69 |
| REFERENCES .....   | 70 |

## List of Figures

|     |  |    |
|-----|--|----|
| 1.1 | Parts of a Plant Vessel.....   | 2  |
| 2.1 | Development of Plant from a Seed.....                                    | 5  |
| 2.2 | Portion of Vessel Element for 5-Pore and 20-Pore Perforation Plates..... | 7  |
| 3.1 | Idealized Xylem with Perforation Plates .....                            | 8  |
| 3.2 | Ideal Velocity Distribution for Laminar Flow .....                       | 11 |
| 3.3 | Laminar Pipe Fluid Flow in a Pipe .....                                  | 13 |
| 3.4 | View of the Pipe .....   | 14 |
| 4.1 | Experimental Setup of the Straight Duct .....                            | 21 |
| 4.2 | Experimental Setup for the 20-Pore Perforation Plate .....               | 22 |
| 5.1 | Friction Factor vs Reynolds Number .....                                 | 34 |
| 5.2 | Loss Coefficient vs Reynolds Number.....                                 | 35 |
| 6.1 | Plot of the Velocity Vectors for the Straight Duct.....                  | 40 |
| 6.2 | Plot of the Pressure Profile for the Straight Duct .....                 | 41 |
| 6.3 | Plot of Stream Lines for a Straight Duct .....                           | 42 |
| 6.4 | Plot of Velocity Vectors for the 5-Pore Perforation Plate .....          | 43 |
|     | 6.4.1 Velocity Vectors Emphasizing Portion A .....                       | 44 |
| 6.5 | Plot of Pressure Profile for the 5-Pore Perforation Plate .....          | 45 |
|     | 6.5.1 Pressure Profile Emphasizing Portion A .....                       | 46 |
| 6.6 | Plot of the Streamlines for the 5-Pore Perforation Plate .....           | 47 |
| 6.7 | Plot of Velocity Vectors for the 20-Pore Perforation Plate.....          | 48 |
|     | 6.7.1 Velocity Vectors Emphasizing Portion B .....                       | 49 |
| 6.8 | Plot of Pressure Profile for the 20-Pore Perforation Plate.....          | 50 |
|     | 6.8.1 Pressure Profile Emphasizing portion B.....                        | 51 |
| 6.9 | Plot of Streamlines for the 20-Pore Perforation Plate .....              | 52 |

## Nomenclature

|                 |  |
|-----------------|--|
| A               | cross-sectional area of the test section                         |
| D               | diameter of the test section                                     |
| f               | friction factor  |
| g               | acceleration due to gravity                                      |
| $H_f$           | head loss in the test section                                    |
| K               | loss coefficient   |
| L               | length of the test section                                       |
| $\Delta p_{os}$ | pressure drop in the pipe due to obstruction and the smooth wall |
| $p_s$           | pressure drop due to the smooth wall of the pipe                 |
| Q               | flowrate   |
| r               | radius of the test section                                       |
| Re              | Reynolds number  |
| $x_L$           | hydrodynamic entry length  |
| V               | average fluid velocity in test section                           |
| Vol             | total volume of fluid  |
| $\Delta t$      | time taken to collect fluid in cylindrical jar                   |
| $u_A$           | uncertainty in cross-sectional area of the tube                  |
| $u_D$           | uncertainty in diameter of the tube                              |
| $u_\rho$        | uncertainty in density of the fluid                              |
| $u_{Hf}$        | uncertainty in head loss   |
| $u_{\Delta H}$  | uncertainty in hydraulic head                                    |
| $u_L$           | uncertainty in length of the test section                        |
| $u_f$           | uncertainty in friction factor                                   |
| $u_{p_s}$       | uncertainty in the pressure drop of the smooth wall              |

|                |                                       |
|----------------|---------------------------------------|
| $u_Q$          | uncertainty in flowrate               |
| $u_{\Delta t}$ | uncertainty in time interval          |
| $u_V$          | uncertainty in velocity               |
| $u_\mu$        | uncertainty in viscosity of the fluid |
| $u_{Vol}$      | uncertainty in volume                 |

### Greek Symbols

|                |                       |
|----------------|-----------------------|
| $\rho_{fluid}$ | density of fluid      |
| $\rho_{cs}$    | density of corn syrup |
| $\mu$          | dynamic viscosity     |
| $\psi$         | streamfunction        |
| $\omega$       | vorticity             |
| $\nabla$       | del operator          |

## **Chapter 1**

### **INTRODUCTION**

#### **1.1 Overview**

Water availability is one of the most important factors limiting the growth of plants throughout the world in both natural and agricultural settings. Without plants and the water that sustains them, life as we know it would not exist. Living organisms originated from an aqueous environment and during their course of evolution they depended upon water in a variety of ways. Water provides a medium for the movement of dissolved substances in plant xylem and phloem. Water also provides some support to fully submerged or partly submerged aquatic plants due to the buoyancy of stems and leaves. Plants are irrigated with water which may be in limited supply, particularly in desert environments. Therefore, one important aspect of plant biology involves an understanding of the use of water by plants.

We must remember that the study of the plant/water relationship has wide implications in many disciplines, ranging from more efficient production of crops to the capacity to control our environment and increase protection from adverse influences. Knowledge in this area will help scientists to predict the use of water by plants and help practitioners to cater to the irrigation needs of specific plants.

For terrestrial plants, survival depends upon the ability to supply their leaves with water acquired by the roots. For this function, plants have evolved specialized conducting tissues and cells. Plant vessels are conduits that are made of individual

cells. At the end of each vessel element there is a remnant of that cell's end wall which is called a "perforation plate" as shown in figure 1.1.

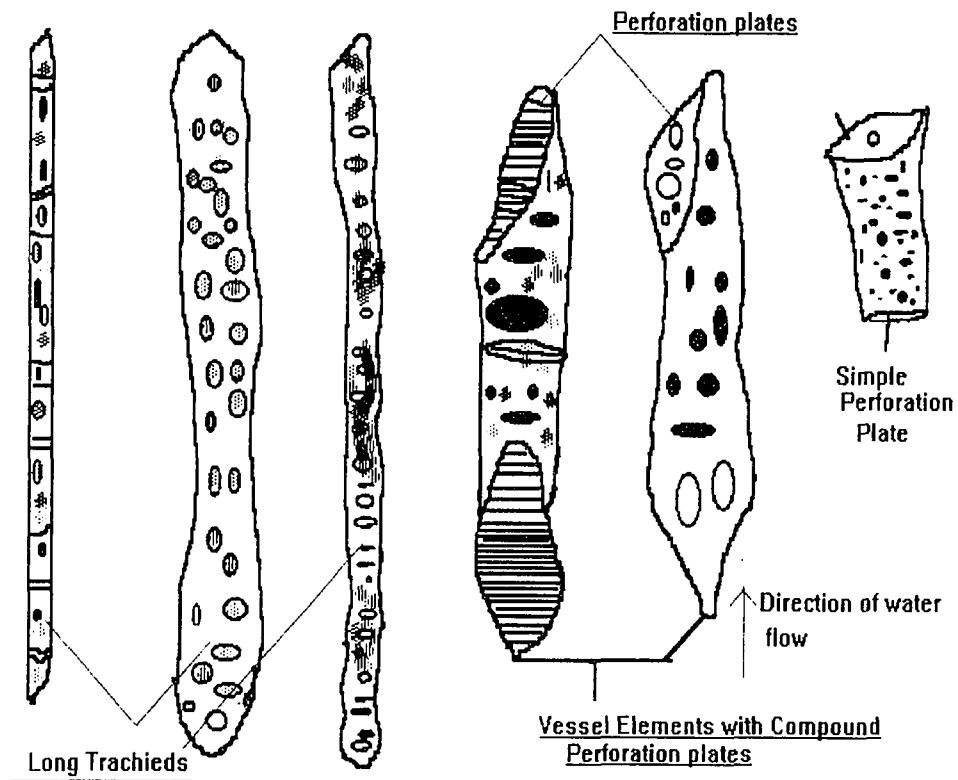


**Figure 1.1 Parts of a Plant Vessel**

In this project, experiments were conducted to study the behavior of water flow in plants with a 5-pore perforation plate and a 20-pore perforation plate. Corn syrup, because of its viscous nature was used as the working fluid in order to match the fluid flow in the xylem portion of plants. The goal of this project was to help understand the role of perforation plates in water flow through plants and to ascertain the importance of fluid mechanics in the plant/water relationship.

Loss coefficients were calculated to determine the role of perforation plates in restricting the flow of water through plant xylem.

Pressures and velocities were measured by conducting experiments with and without perforation plates. These values were compared with numerical values obtained using NEKTON, a computational fluid dynamics package. Computer modeling also assisted in visualizing flow through the pores of the perforation plates.

## Chapter 2

### REVIEW OF PAST WORK

#### 2.1 Literature Review

Modeling the flow of water through plants has been a popular topic in recent years. Many researchers have approached various aspects of fluid flow through plants with varying results. The role of xylem, or water conducting ducts in plants, is to transport water from the roots of a plant as shown in the figure 2.1 up through the stem and to the leaves or to the growing end of plant. The ascent of water in trees was studied by Ewart (1904). He found that the flow of water through open vessels filled with sap obeyed Poiseuille's equation. His estimates of the amount of flow were made from the flowrate, diameter, and the number of vessels. His data showed that the actual flow in dicotyledonous plants took place through the vessels as shown in figure 1.1. He found that large vessels offered much less resistance to flow than the more abundant narrow vessels, though both vessels had the same total cross-sectional area.

Flow in xylem vessels was examined by Giordano (1977). He measured the flow of water in xylem vessels at various pressures and concluded that Poiseuille's equation could not be used across perforation plates because the fluid flow changed abruptly across these plates and did not have a chance to become fully-developed. As seen in figure 3.1 perforation plates are cell wall remnants in the cells within a plant that form plant xylem. These cells interconnect at the perforation plates to form the long, thin conduits that provide a path for water flow through the plant. To prove this, he conducted an experiment and found that Poiseuille's equation could not describe the

entry region under his experimental conditions since the relationship between the flowrate and applied pressure was neither linear nor monotonic. Also, the magnitude of the flowrate was lower than that would have been expected from measured pressure differences.

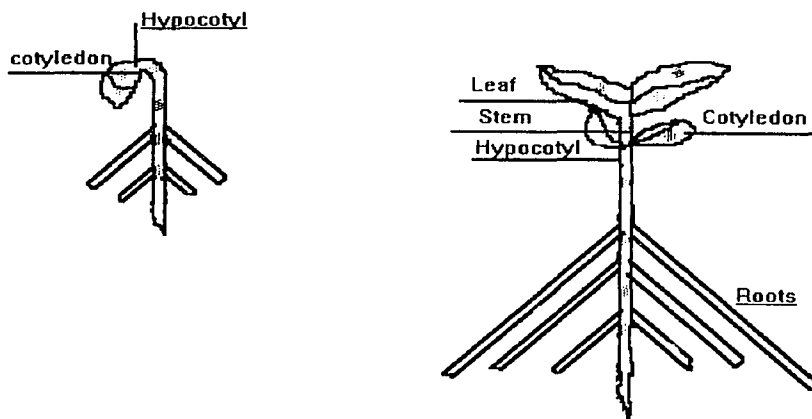


**Figure 2.1 Development of a Plant from a Seed**

The ascent of sap in plants was reviewed by Pickard (1981). He discussed the validity of the Hagen-Poiseuille equation, end-effects caused by the perforation plates, and the effect of creeping flow. The Hagen-Poiseuille equation sufficed to give the pressure drop along the impermeable tracheary element unless there were large variations in the cross-section of the perforation plate. Under these circumstances, it was also difficult to measure the pressure drop. While discussing the end effects, he explained that the problem of the perforation plates could be avoided by assuming that the perforation plate could be treated as an orifice in a thin diaphragm stretched across the pipe or xylem. He cited previous experimental research as justification for his

conclusions. He also found that when the perforation plate diameter approached the vessel diameter, the pressure drop became small.

The hydraulic conductance of vessels in plants was studied by Schulte (1989) using five species of dicotyledons that had simple or compound perforation plates. Measured conductance showed agreement with predicted values from the Hagen-Poiseuille equation for flow through ideal capillaries. He developed a physical analog model with and without perforation plates and found that there was little flow reduction

Water flow through vessel perforation plates was also studied by Schulte (1993) using a numerical approach employing the computational fluid dynamics package, FIDAP, to study flow through plant vessels. He modeled the fluid flow in vessels with and without a perforation plate to study the effect on pressure drop. His studies included a 5-pore perforation plate for the plant *Liriodendron tulipifera* as shown in figure 2.2. He concluded that the perforation plates did not create any significant obstruction to the flow of water and suggested that more analyses were needed for more complicated plates with 20 or more pores.

Additional modeling studies have been done on fluid flow through perforation plates by Schulte (1993). At this time he studied the effects of perforation plate thickness and plate angle on fluid flow using his computational fluid model. In this study he found that the pressure gradient increased as the plate thickness and the plate angle was increased. At the same time he found that the velocity profile also changed across the vessel as the plate angle and the size of the pore was changed. He suggested that if the xylem vessel was considered as an inert conduit for water flow, these changes would be unimportant.

This review of past work has discussed the various types of modeling that have been done on the flow of water in plant vessels. In the current research, an experimental study of the flow in plants vessels was conducted. First, experiments

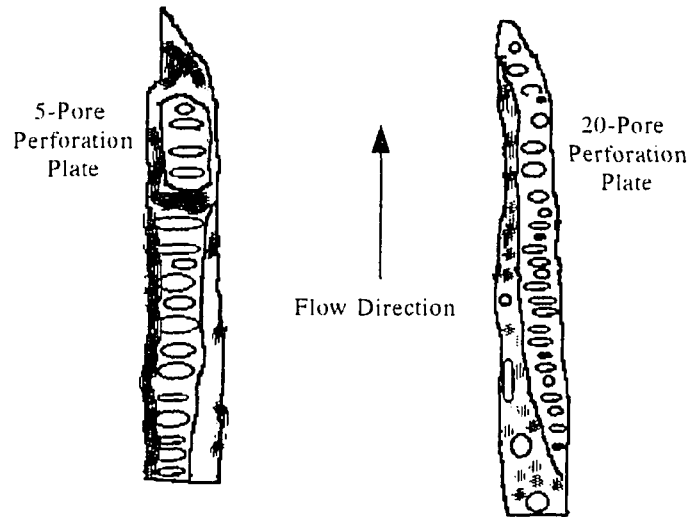


**Figure 2.2 Portion of Vessel Element for 5-Pore and 20-Pore Perforation Plates**

were conducted in the laboratory using a straight duct. Next, obstruction plates were inserted into the duct to model flow through plant vessel perforation plates. Experiments were done for a straight duct, a duct with a 5-pore perforation plate, and a 20-pore plate to measure pressure losses across the plates. These experimental results were compared with the numerical model developed by P. J. Schulte. Next, NEKTON, a computational fluid dynamics package installed on a Silicon Graphics workstation located at the National Supercomputing Center for Energy and the Environment at UNLV was used to verify the behavior of the fluid flow.

## Chapter 3

### THEORETICAL DESCRIPTION

#### 3.1 Stokes Flow

Stokes, while studying the flow past a sphere, found that his law describing the flow of fluids at low velocities was valid only if the Reynolds number was less than one. The typical flow through the xylem of a typical plant stem with the diameter of  $30\ \mu\text{m}$  has a Reynolds number of 0.05. In the present work, xylem was modeled

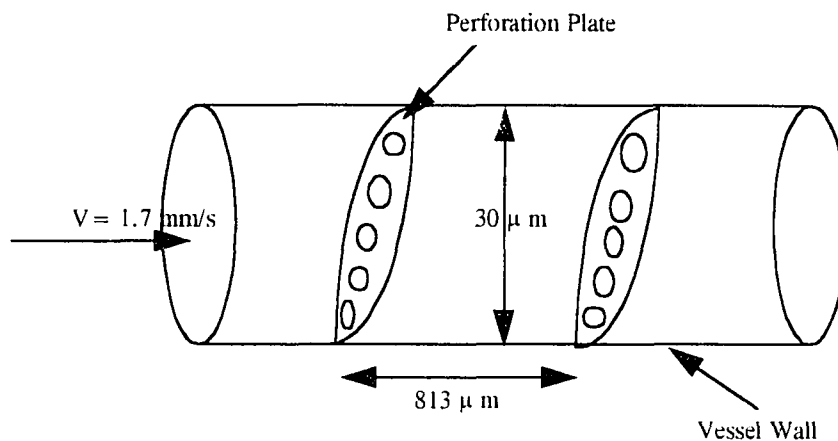


**Figure 3.1 Idealized Xylem with Perforation Plates**

as a circular pipe of intermediate length with an angled perforation plate crossing the pipe at an angle of approximately 20 degrees. The geometry is shown in the figure 3.1. Average distance between the perforation plates in the figure 3.1 is

813  $\mu\text{m}$ . For low Reynolds number flows, viscous forces dominate over inertial forces since the velocity is small.

When the inertia terms are neglected from the equations of motion, the resulting solution will be valid for Reynolds numbers of less than one. Such a flow is referred to as creeping flow, or the motion is called creeping motion.

The Navier-Stokes equations for an incompressible fluid flow in vector notation is given by:

$$\rho \frac{d\vec{V}}{dt} = -\vec{\nabla}p + \vec{F} + \mu \vec{\nabla}^2 \vec{V} \quad (1)$$

If inertial terms are neglected for low Reynolds numbers, and body forces are not present, the incompressible Navier-Stokes equation reduces to:

$$\vec{\nabla}p = \mu \vec{\nabla}^2 \vec{V} \quad (2)$$

With using the vector identity:

$$\vec{\nabla} \times (\vec{\nabla} \times \vec{V}) = \vec{\nabla} \cdot (\vec{\nabla} \cdot \vec{V}) - \vec{\nabla}^2 \vec{V} \quad (3)$$

$$\vec{\nabla} \times \vec{V} = \vec{\omega}, \quad \text{where } \vec{\omega} = -\vec{\nabla}^2 \Psi \quad (4)$$

The divergence of the velocity vector is defined as:

$$\vec{\nabla} \cdot \vec{V} = \text{divergence of } \vec{V} \quad (5)$$

From continuity, the divergence of velocity for a steady, incompressible fluid is equal to zero. Substituting equation 3 in equation 2 will result in:

$$\vec{\nabla}p = \mu(-\vec{\nabla} \times (\vec{\nabla} \times \vec{V})) \quad (6)$$

Taking the curl of equation 6:

$$\vec{\nabla} \times (\vec{\nabla} p) = \mu \vec{\nabla} \times (-\vec{\nabla} \times \vec{\omega}) \quad (7)$$

Also,  $\nabla \times \nabla p = 0$  by vector identity. Substituting this identity into equation 7:

$$-\mu \vec{\nabla} \times (\vec{\nabla} \times \vec{\omega}) = 0 \quad (8)$$

$$\vec{\nabla} \times (\vec{\nabla} \times \vec{\omega}) = \vec{\nabla}(\vec{\nabla} \cdot \vec{\omega}) - \nabla^2 \vec{\omega} \quad (9)$$

Also, by substituting these conditions into equation 9 will result in the following expression:

$$\nabla^2 \vec{\omega} = 0 \quad (10)$$

Substituting the value of  $\omega$  into equation 10 will give an expression for the streamfunction for a Stokes flow as follows:

$$\nabla^4 \Psi = 0 \quad (11)$$

Equation 11 shows that the equation of a plane creeping motion is a biharmonic function which shares many of the same properties as Laplace's equation. Inviscid, incompressible, irrotational flow fields are governed by Laplace's equation and are commonly called potential flow. As Laplace's equation is linear, any number of particular solutions can be added together to obtain other solutions.

### 3.2 Velocity Distribution through the Cross-section of a Pipe.

To study the velocity distribution of a laminar flow in circular pipes, velocity may be plotted versus radial position as shown in figure 3.2. Over the diameter

of the pipe. the resulting curve will describe a parabola with peak velocity occurring along the central axis of the pipe.

The velocity at any distance  $r$  from the central axis of the pipe is given by

$$u = \frac{\Delta p}{4L\mu} \left[ \frac{D^2}{4} - r^2 \right] \quad (12)$$

The velocity is maximum at  $r = 0$  where equation 12 reduces to:

$$u_{\max} = \frac{\Delta p}{4L\mu} \left[ \frac{D^2}{4} \right] \quad (13)$$

The velocity distribution can be written in terms of  $u_{\max}$  as:

$$\frac{u}{u_{\max}} = 1 - \left( \frac{4r^2}{D^2} \right) \quad (14)$$

Equation 14 also describe a parabolic velocity distribution.

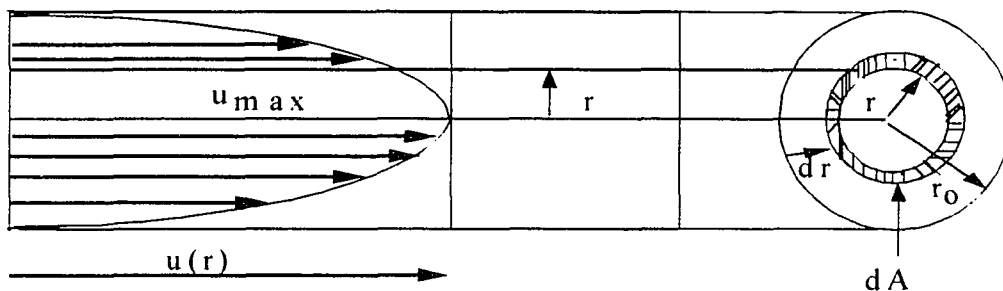


**Figure 3.2 Ideal Velocity Distribution for Laminar Flow**

A fully-developed parabolic velocity distribution exists only at a considerable distance downstream from the entrance of a pipe. This hydrodynamic entry length can be calculated using the following correlation (White, 1991):

$$\frac{x_L}{D} \approx \frac{0.6}{1.0 + 0.035 \text{Re}_D} + 0.056 \text{Re}_D \quad (15)$$

$x_L$  entrance length

$\text{Re}_D$  Reynolds number

$D$  hydraulic diameter

From equation 15, the entrance length ( $x_L$ ) will not vanish as  $\text{Re}$  approaches zero. It takes about 0.6 diameters for a creeping flow to change from a uniform to a parabolic profile. This equation is used to calculate the hydrodynamic entry length in case of laminar flow only, it is valid for Reynolds numbers between 0 and 2300. The velocity distribution is altered if there is a change in the alignment of the pipe or if an obstruction is placed in the flow. Any change in the velocity distribution will alter the power required to force the fluid through the pipe and affect the pressure resistance to the flow.

### 3.3 Hagen-Poiseuille Flow

Some of the earliest studies in the field of viscous flow were experimental investigations of laminar flow in straight pipes of a circular cross-section. This work was conducted by two researchers: Hagen experimented with water flow through tubes, and Poiseuille studied the behavior of blood as it flowed through the veins of the body.

#### 3.3.1 Derivation of Hagen-Poiseuille Equation

Consider a straight pipe of internal diameter  $D$ . It is assumed that the flow is

steady and laminar. When the fluid flows in the pipe as shown in figure 3.3, a cylindrical portion of the fluid is subjected to the sum of the indicated forces as shown in figure 3.4.

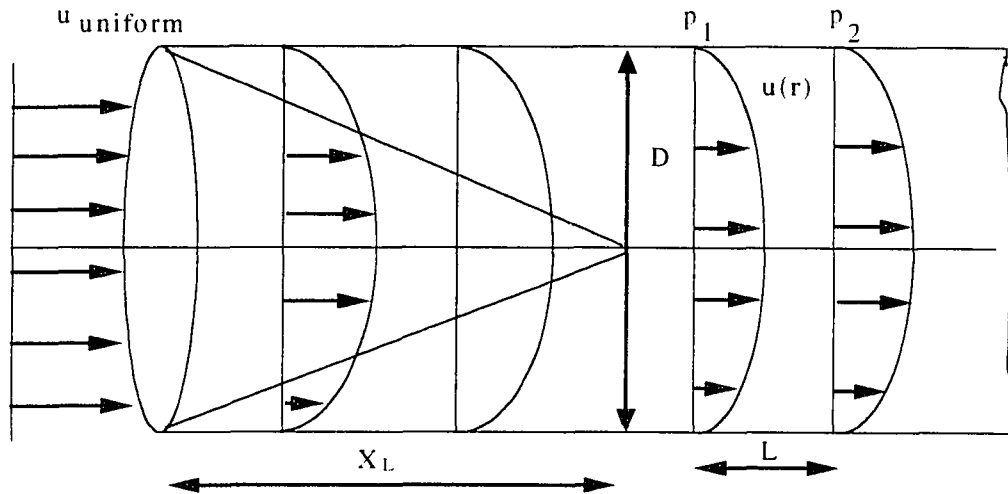


**Figure 3.3 Laminar Fluid Flow in a Pipe**

If the fluid moves from left to right, the force on the cylindrical section of fluid in the direction of the flow produced by the pressure difference is:

$$(p_1 - p_2) \frac{\pi D^2}{4} \quad (16)$$

The average velocity will not change along the axis of the pipe and there is no accelerating force acting on the fluid particles. Shear stresses due to fluid viscosity still act on the outer surface of the cylinder wall.

The total shear force on the outside of the cylinder is the product of the shear stress and the area of this cylindrical surface. It is equal to:

$$-\mu(\pi D L) \frac{du}{dr} \Big|_{r_0} \quad (17)$$

The negative sign indicates that the shear force opposes the direction of flow. The cylindrical fluid body is in a uniform motion, which is the condition for equilibrium.

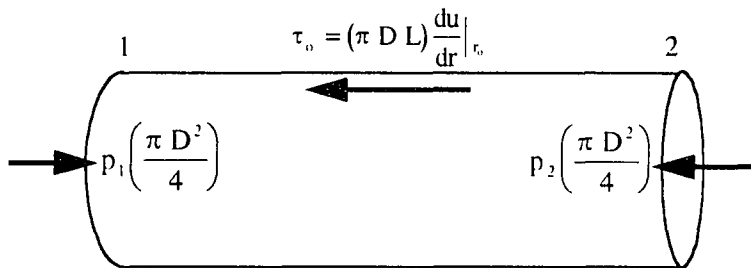


**Figure 3.4 View of the Pipe**

According to the condition of the equilibrium, the sum of the axial forces should be zero. Equating equations 16 and 17:

$$(p_1 - p_2) \frac{\pi D^2}{4} = -\mu \frac{du}{dr} (\pi D L) \quad (18)$$

This can be simplified by expressing it in the form of the following differential equation:

$$\frac{du}{dr} = -\frac{(p_1 - p_2) D}{4 \mu L} \quad (19)$$

Equation 19 is integrated, leaving one constant of integration:

$$u = -\frac{(p_1 - p_2) D^2}{16 \mu L} + A \quad (20)$$

By assuming the no-slip boundary condition and specifying that  $u(r)=0$  at  $r = 0$ , the constant of integration,  $A$ , is determined. If we input these values in equation 19, we obtain the equation for the velocity at any point:

$$u(r) = \frac{(p_1 - p_2)}{4 \mu L} \left[ \frac{D^2}{4} - r^2 \right] \quad (21)$$

Equation 21 indicates that the velocity is distributed in the form of a parabola. The average velocity,  $V_g$ , is given by:

$$V_g = \frac{4}{\pi D^2} \int_0^{D/2} u(r) 2 \pi r dr \quad (22)$$

By substituting equation 21 into 22, an equation for the average velocity is obtained and is given as following equation:

$$V_g = \frac{(p_1 - p_2) D^2}{32 \mu L} \quad (23)$$

The discharge of a fluid passing through any section per unit time is the product of the average velocity and the area:

$$Q = \frac{\pi(p_1 - p_2) D^4}{128 \mu L} \quad (24)$$

Equation 24 is the classic Hagen-Poiseuille equation. In terms of the pressure difference the Hagen-Poiseuille equation is written as:

$$\Delta p = \frac{128 Q \mu L}{\pi D^4} \quad (25)$$

### 3.4 Minor Losses

In the design of pipelines, energy loss due to friction becomes the dominant factor for long pipes. Losses in elbows, valves and fittings may be equal to or greater than the frictional losses. In piping systems, the losses due to flow past these small obstructions are known as minor losses. The flow pattern in fittings and valves is quite complex. The pressure losses in fittings and valves have been measured experimentally and the results have been correlated with the available pipe-flow parameters. In the case of valves, the flow pressure drop relation depends on the manufacturer's design. In order to calculate the losses in valve design, estimates must be taken from manufacturers' tables. Minor loss coefficients are usually given as the ratio of the head loss through the device to the velocity head of the piping system. The loss coefficient,  $K$ , is given as:

$$K = \frac{\Delta p}{0.5 \rho V^2} \quad (26)$$

where  $K$  is a dimensionless parameter. As an example the loss coefficient for a 90 degree elbow in a piping system is approximately 0.9. A single piping system often has many minor losses and all of these losses are correlated to the velocity head. If the pipe system has a constant diameter, the losses are summed together and given as total system loss. If the pipe diameter varies, the velocity head changes and the losses should be calculated separately.

In the straight pipe pressure drop is computed from the head loss:

$$H_f = \frac{f L V^2}{2 g D} \quad (27)$$

$H_f$  head loss in the pipe (m)

|   |   |
|---|---|
| f | friction factor                                 |
| L | length of the test section (m)                  |
| D | diameter of the test section (m)                |
| g | acceleration due to gravity (m/s <sup>2</sup> ) |

For laminar flow,  $f=64/Re_D$ .

If a perforation plate is inserted in the straight pipe, there will be some losses due to this obstruction and the head loss can be computed using the following equation:

$$H_f = \frac{K V^2}{2g} \quad (28)$$

K loss coefficient

To model the plant xylem discussed at the beginning of the chapter 3, the pressure drop across a 813  $\mu\text{m}$  section of pipe with one 20-pore perforation plate or a 5-pore perforation plate with  $Re=0.66$  is given in the table 3.1.

| Re=0.66                      | 5-Pore Perforation Plate |    | 20-Pore Perforation Plate |    |
|------------------------------|--------------------------|----|---------------------------|----|
|                              | Pa                       | %  | Pa                        | %  |
| $\Delta p$ pipe wall         | 3.79                     | 64 | 3.79                      | 4  |
| $\Delta p$ perforation plate | 2.16                     | 36 | 85                        | 96 |
| $\Delta p$ total             | 5.95                     |    | 88.79                     |    |

**Table 3.1 Pressure Drop for a Model of the Xylem Portion of a Plant**

The loss coefficient for minor losses in equation 28 can be compared to the friction factor for straight pipes in equation 27:

$$H_f = \frac{f L V^2}{2 g D} = K \frac{V^2}{2 g}$$

From the comparison of equations 27 and 28, equation 29 is obtained and is given as following:

$$K = f \frac{L}{D} \quad (29)$$

The pressure drop due to a total head loss of  $H_f$  can be found from:

$$\Delta p = \rho g H_f \quad (30)$$

The power required to pump a fluid against a head loss of  $H_f$  is given by:

$$\text{power} = \dot{m} g H_f \quad (31)$$

## Chapter 4

### EXPERIMENTAL SETUP AND PROCEDURE

#### 4.1 Overview

The present study was undertaken to gain an understanding of water flow in plant xylem. The objective of this study was to measure the flow of water through perforation plates that modeled actual plant xylem. Flow was modeled using corn syrup as the working fluid.

#### 4.2 Experimental Setup

An experimental apparatus was constructed in the Fluid Mechanics Laboratory at UNLV to measure the pressure drop across multi-pore perforation plates in circular ducts. The size of the setup and the choice of a working fluid were decided upon by modeling an actual plant xylem. Xylem from the *Liriodendron tulipifera* (tulip tree) plant was modeled using a 5-pore perforation plate. A 20-pore perforation plate was used to model the xylem portion of *Liquidambar styraciflua* (sweetgum). The duct size for the experiment was chosen to match the Reynolds number of the flow and to permit the use of commercially-sized plexiglas pipe. A duct inner diameter of 38.1 mm (1.5 in) was chosen to be a practical size for machining appropriate perforation plates, but a suitable working fluid had to be chosen to match the Reynolds numbers predicted for actual plant xylem flows.

#### **4.2.1 Working Fluid**

In order to match the low Reynolds number found in plant xylem, flow calculations were made to check the fluid properties of water and corn syrup. Corn syrup, due to its large kinematic viscosity was found to be an ideal fluid for matching the Reynolds number of the flow. The properties of corn syrup were obtained from the Critical Databook (1984). Variation of the viscosity was significant in the present study as the corn syrup dried out quickly when exposed to air. The viscosity of the fluid was first measured using the ball method. Ball bearings with a diameter of 4.32 mm were dropped through the fluid from a height of about 180 mm, and the time was noted for the ball bearing to reach the bottom of the jar. Using the Stokes equation, the viscosity was calculated but the Reynolds number exceeded the Stokes range. The viscosity was later determined directly from experiments which produced values that fell into the range of viscosities for corn syrup available from the Critical Databook (1984). During each experiment, viscosity was found by measuring the pressure drop across a fixed length of a circular pipe and by using the Hagen-Poiseuille equation for laminar flow.

#### **4.2.2 Description of the Experimental Setup**

Schematic views of the test section are shown in figure 4.1. and 4.2. The setup consisted of a bucket mounted on dexion bars about 1830 mm above the ground. These dexion bars were supported on a table. The purpose of the bucket was to store the corn syrup to run the experiment and to provide a fixed hydraulic head. PVC pipes were used to connect the test section and the bucket. Two brass valves, 38.1 mm in diameter were used to regulate the flow at the inlet and outlet. A clear Plexiglas tube was used as the test section. The inside diameter of the

Plexiglas tube was 38.1 mm and the outside diameter was 50.8 mm. PVC schedule 40 pipe was used to connect the test section to the inlet and outlet.

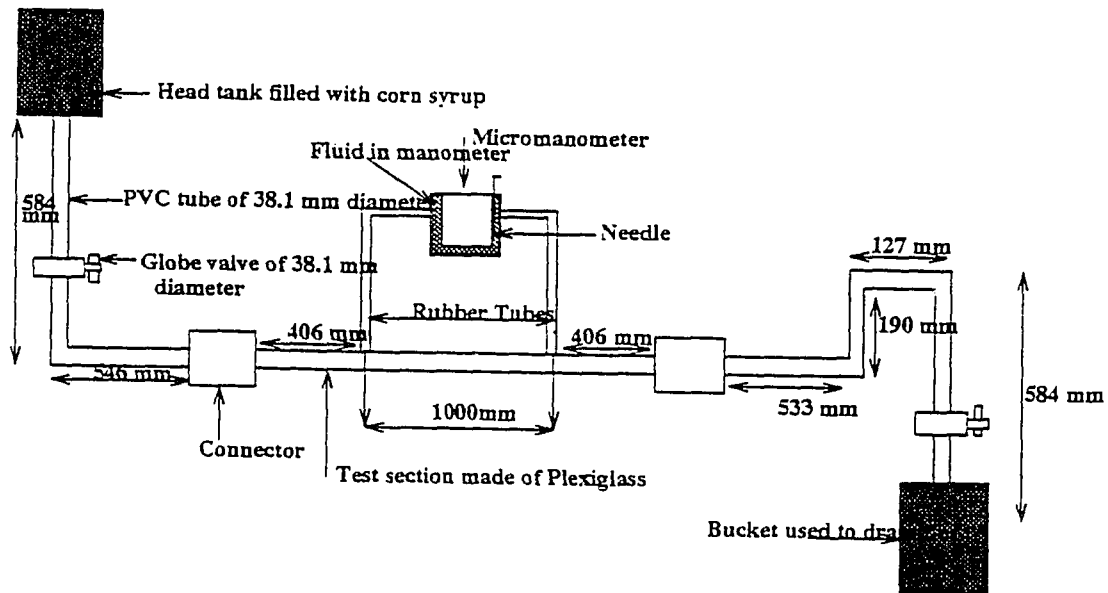


Figure 4.1 Experimental Setup for the Straight Duct

The diameter of the test section used was 38.1 mm to match the diameter of the inlet section. The test section was connected using smooth-walled couplings. Care was taken to prevent any leakage in the setup.

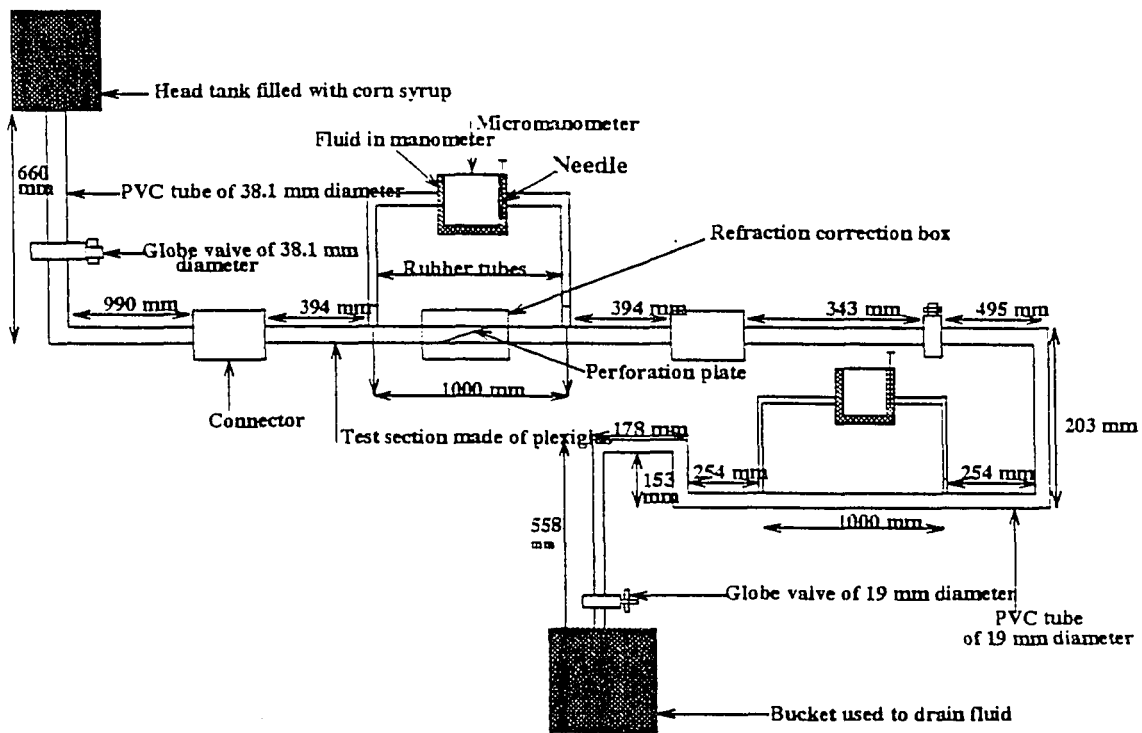


Figure 4.2 Experimental Setup for the 20-Pore Perforation Plate

### 4.2.3 Instrumentation

A Dwyer micromanometer was used to measure the pressure drop across the test section. The pressure drop was measured between two points placed 1 meter apart. Rubber tubes were connected to the pressure taps placed on either side of the test section. The diameter of the rubber tubes was 6.4 mm. Graduated cylindrical jars were used to collect the corn syrup and to determine the volume of the fluid. A stopwatch was used to measure the time taken to collect the corn syrup in the jar. Buckets were used to store the corn syrup before and after running the experiments. Care was taken to prevent the corn syrup from drying out by covering the bucket with the plastic after every trial.

### 4.3 Experimental Procedure

To begin the experiment, the head tank was filled with corn syrup and it was allowed to settle for about half hour so that the air bubbles could rise to the surface. Once the corn syrup settled, the inlet valve was opened and the fluid was allowed to flow. When steady flow was achieved, the inlet valve was closed and a zero reading was taken on the micromanometer. Next the inlet valve was opened and the fluid was allowed to pass through the test section. When the fluid started moving, a final manometer reading was taken. The difference in the zero reading and the final reading gave the pressure drop between the two points. At the same time, some amount of fluid was collected in a graduated cylinder and the time taken to fill the cylinder was also noted. Knowing the time and the volume, the volumetric flowrate was calculated. The same procedure was repeated with different valve openings to get different values of pressure drop and flowrates.

Using these flowrates, the velocity and the Reynolds number was calculated each time.

$$Q = \frac{\text{Vol}}{\Delta t} \quad (1)$$

where,

|            |   |
|------------|---|
| Vol        | volume of the fluid (m <sup>3</sup> )               |
| $\Delta t$ | time taken to collect the fluid (s)                 |
| Q          | flowrate $\left(\frac{\text{m}^3}{\text{s}}\right)$ |

$$V = \frac{Q}{A} \quad (2)$$

|   |  |
|---|--|
| V | velocity of fluid flow in test section                     |
| A | cross-sectional area of the test section (m <sup>2</sup> ) |

For the 5-pore and 20-pore perforation plate experiments, an additional section of the pipe was added after the test section to measure the viscosity of the fluid. This was necessary since the corn syrup had a tendency to dry out which caused the viscosity to vary daily. The pressure drop across a one meter section of the pipe was measured with a micromanometer to provide the viscosity from the Hagen-Poiseuille equation:

$$\mu = \frac{\rho_{\text{fluid}} g \Delta H D^2}{32 L V} \quad (3)$$

|                       |   |
|-----------------------|---|
| $\mu$                 | dynamic viscosity (kg / m-s)            |
| $\rho_{\text{fluid}}$ | density of fluid (kg / m <sup>3</sup> ) |

|            |   |
|------------|---|
| $g$        | acceleration due to gravity (m / s <sup>2</sup> ) |
| $\Delta H$ | measured drop in hydraulic head ( m of water)     |
| $D$        | diameter of the test section (m)                  |
| $L$        | length of the test section (m)                    |
| $V$        | velocity in the test section (m / s)              |

$$Re = \frac{\rho_{cs} V D}{\mu} \quad (4)$$

|             |  |
|-------------|--|
| $Re$        | Reynolds number                              |
| $\rho_{cs}$ | density of corn syrup (kg / m <sup>3</sup> ) |

Experiments were conducted in a straight section of pipe to verify the expected relationship for the friction factor in the pipe:

$$f = \frac{64}{Re} \quad (5)$$

Next, a 5-pore perforation plate was added to the pipe and the pressure drop was measured as indicated earlier. Then, a 20-pore perforation plate was added to the pipe and the pressure drop was measured across the perforation plate, with the addition of a straight pipe to measure viscosity for every trial. The following equations were used to calculate the pressure drop due to the obstruction caused by the perforation plate in the pipe. First the pressure drop in the pipe due to the obstruction and the smooth wall was calculated.

$$\Delta p_{os} = \rho_{water} g \Delta H \quad (6)$$

$\Delta p_{os}$  pressure drop due the obstruction and the smooth wall (Pa)

$\Delta H$  measured hydraulic head (m)

To find the head loss in the pipe:

$$H_f = \frac{f L V^2}{2 g D} \quad (7)$$

$H_f$  head loss in the pipe (m)

To find the pressure drop of the smooth wall of the pipe alone:

$$\Delta p_s = \rho_{cs} g H_f \quad (8)$$

$\Delta p_s$  pressure drop due to the smooth wall of the pipe (Pa)

Subtracting the equation (8) from (6) gave the pressure drop due to the obstruction alone.

#### 4.4 Uncertainty Analysis

An uncertainty analysis of the data was performed to estimate errors, and the general validity of the experimental measurements. An uncertainty analysis helped to indicate the overall accuracy of a measurement by identifying certain critical variables in the measurement process. The Kline and McClintock method (Holman, 1978) was adopted to determine the uncertainties in the viscosity, Reynolds number, pressure, and the loss coefficient. This method is based on the specification of the uncertainties in the various primary experimental measurements, and is based on the following relationship.

For  $R = R(x_1, x_2, x_3, \dots, x_n)$ , let  $w_R$  be the uncertainty in the result and  $w_1, w_2, \dots, w_n$  be the uncertainties in the independent variables,  $x_1, x_2, \dots, x_n$ . If the uncertainties in the independent variables are known, then the uncertainty in the result  $R$  is given by the following relation:

$$w_R = \sqrt{\left(\frac{\partial R}{\partial x_1} w_1\right)^2 + \left(\frac{\partial R}{\partial x_2} w_2\right)^2 + \dots + \left(\frac{\partial R}{\partial x_n} w_n\right)^2} \quad (9)$$

To compute the uncertainty in the flowrate:

$$u_Q = Q \sqrt{\left(\frac{u_{Vol}}{Vol}\right)^2 + \left(\frac{u_{\Delta t}}{\Delta t}\right)^2} \quad (10)$$

- $u_Q$       uncertainty in flowrate
- $u_{Vol}$     uncertainty in volume
- $Vol$       total volume of the fluid
- $u_{\Delta t}$     uncertainty in time interval
- $\Delta t$       time taken to collect the fluid in the cylindrical jar

To compute the uncertainty in the area of the small tube:

$$u_{A_t} = A_t \sqrt{\left(\frac{u_{D_t}}{D_t}\right)^2} \quad (11)$$

- $u_{A_t}$     uncertainty in cross-sectional area of the tube
- $A_t$       cross-sectional area of the tube
- $u_{D_t}$     uncertainty in the diameter of the tube
- $D_t$       diameter of the tube

To compute the uncertainty in the velocity through the tube:

$$u_{v_t} = V_t \sqrt{\left(\frac{u_{Q_t}}{Q_t}\right)^2 + \left(\frac{u_{A_t}}{A_t}\right)^2} \quad (12)$$

$u_{v_t}$  uncertainty in the velocity of the flow through the small tube

$V_t$  velocity of the flow in the small tube

To compute the uncertainty in the viscosity of the fluid:

$$u_{\mu} = \mu \sqrt{\left(\frac{u_{D_t}}{D_t}\right)^2 + \left(\frac{u_{L_s}}{L_s}\right)^2 + \left(\frac{u_{v_t}}{V_t}\right)^2 + \left(\frac{u_{\Delta H}}{\Delta H}\right)^2} \quad (13)$$

$u_{\mu}$  uncertainty in the viscosity of the fluid

$u_{L_s}$  uncertainty in the length of the tube

$u_{\Delta H}$  uncertainty in the deflection of the manometer

$\Delta H$  deflection in the manometer

$L_s$  length of small tube

To find the uncertainty in the Reynolds number :

$$u_{Re} = Re \sqrt{\left(\frac{u_{\rho}}{\rho}\right)^2 + \left(\frac{u_V}{V}\right)^2 + \left(\frac{u_D}{D}\right)^2 + \left(\frac{u_{\mu}}{\mu}\right)^2} \quad (14)$$

$u_{Re}$  uncertainty in the Reynolds number

$Re$  Reynolds number

$u_{\rho}$  uncertainty in the density of the fluid

$\rho$  density of the fluid

To find the uncertainty in the friction factor:

$$u_f = f \sqrt{\left(\frac{u_{Re}}{Re}\right)^2} \quad (15)$$

$u_f$       uncertainty in the friction factor  
 $f$         friction factor

To find the uncertainty in the head loss in the test section:

$$u_{H_r} = H_r \sqrt{\left(\frac{u_f}{f}\right)^2 + \left(\frac{u_L}{L}\right)^2 + \left(2 \frac{u_V}{V}\right)^2 + \left(\frac{u_D}{D}\right)^2} \quad (16)$$

$H_r$       head loss in the test section

To find the uncertainty in the pressure drop of the smooth wall:

$$u_{p_s} = p_s \sqrt{\left(\frac{u_p}{\rho}\right)^2 + \left(\frac{u_{H_r}}{H_r}\right)^2} \quad (17)$$

$u_{p_s}$     uncertainty in the pressure drop of the smooth wall  
 $p_s$       pressure drop of the smooth wall

To compute the pressure drop of the smooth wall plus the obstruction wall:

$$u_{p_o} = p_o \sqrt{\left(\frac{u_{H_r}}{H}\right)^2} \quad (18)$$

- $u_{p_0}$  uncertainty in the pressure drop of the smooth wall plus the obstruction
- $p_0$  pressure drop due to the smooth wall plus the obstruction

To find the uncertainty in the loss coefficient:

$$u_K = K \sqrt{\left(\frac{u_{p_0}}{p_0}\right)^2 + \left(\frac{u_p}{\rho}\right)^2 + \left(-2 \frac{u_v}{V}\right)^2} \quad (19)$$

- $u_K$  uncertainty in loss coefficient
- $K$  loss coefficient
- $u_p$  uncertainty in pressure drop due to obstruction
- $p_0$  pressure drop due to obstruction

The individual variable uncertainties were determined from the instrumentation used in the laboratory and these uncertainties were used to calculate the uncertainty in the flowrate, velocity, viscosity, Reynolds number, and pressure drop for every run. Uncertainties in friction factor and loss coefficient were portrayed as error bars on plots involving these functions and are included in the results.

## Chapter 5

### RESULTS

#### 5.1 Experimental Results: Straight Duct

The first experiment was done with a straight pipe without any obstruction to verify that the working fluid behaved as a Newtonian fluid and to verify that the experimental setup was working properly. The experimental setup shown in figure 4.1 was used. In these experiments, corn syrup was used as the working fluid since it allowed the Reynolds number of the flow to be matched with that of plant xylem in the prototype because of its viscous nature. The density of corn syrup was measured as  $1394 \pm 10 \text{ kg/m}^3$ . The viscosity for corn syrup averaged  $0.120 \pm 0.013 \text{ kg/m-s}$ . Pressure drops and flowrates were obtained from the experiments and these values were used to find the viscosity, Reynolds number and the friction factor. Theoretical friction factors were calculated and a graph was plotted with friction factor versus the Reynolds number. The graph is shown in figure 5.1. The graph was compared to the theoretical value of  $f=64/Re$  for laminar flow. The comparison showed that corn syrup behaved as a Newtonian fluid. It was observed that as the Reynolds number of the flow increased, there was a drop in the friction factor in the pipe. The straight line in friction factor versus Reynolds number for straight duct (figure 5.1) corresponds to  $f=64/Re$ . Tabulated results for all experiments are included in Appendix II.

## 5.2 Experimental Results: 5-Pore Perforation Plate

In this experiment, the effect of a perforation plate on the fluid flow in plant xylem was studied by placing a perforation plate with five pores into straight duct. The perforation plate was placed at an angle of 23 degrees. Corn syrup was once again used as the working fluid in order to match the Reynolds number of the flow in plant xylem. Pressure drop due to the obstruction, flowrate, and viscosity were calculated from the experiments and these values were used to find the loss coefficient and the Reynolds number. The average loss coefficient calculated from the experiment was 8947, while the value obtained from table 3 of the numerical study by (Schulte, 1993) was 8928. The measured range of viscosity was between 0.3 and 0.5 kg/m-s. Contrary to our expectations, pressure drops measured were very small and this caused problems in determining the loss coefficient. Further analysis of the fluid flow through the perforation plates was carried in the third experiment for the more realistic case of a 20-pore perforation plate.

## 5.3 Experimental Results: 20-Pore Perforation Plate

In addition to the 5-pore plate, 20-pore perforation plate experiments were conducted. In this experiment a perforation plate with 20 pores was placed as an obstruction in a straight duct. The perforation plate was placed at an angle of 12.7 degrees. Corn syrup was again used as the working fluid in this experiment. In this experiment, apart from the 38.1 mm (1.5 inch) ID pipe, another pipe of 19 mm (0.75 inch) ID was used to calculate the viscosity of the fluid as shown in the figure 4.2. The average viscosity was  $0.15 \pm 0.017$  kg/m-s. Pressure drops due to the obstruction, flowrate, and the viscosity values were calculated from the experiment. As expected, pressure drops due to the obstruction were very high. Loss coefficients and Reynolds numbers were calculated and the data were plotted as shown in Figure 5.2. The values of the loss coefficient obtained were very high

because of the low velocities. Regression was done using a power fit and an arithmetic average fit. The value of the loss coefficient obtained from the arithmetic average was:

$$K = 86,300 \quad (1)$$

The standard error and the maximum error for the arithmetic fit were 13,700 and 41,900, respectively. The value of the loss coefficient obtained from the power fit was:

$$K = 44,160 \left( \text{Re}^{-0.6871644} \right) \quad R^2 = 0.77 \quad (2)$$

The standard error and the maximum error for the power fit were 5,800 and 12,700 respectively. The experimental setup limited the maximum Reynolds number to 0.5. As seen in figure 5.2, the uncertainty in the measurements as shown by the error bars was very small.

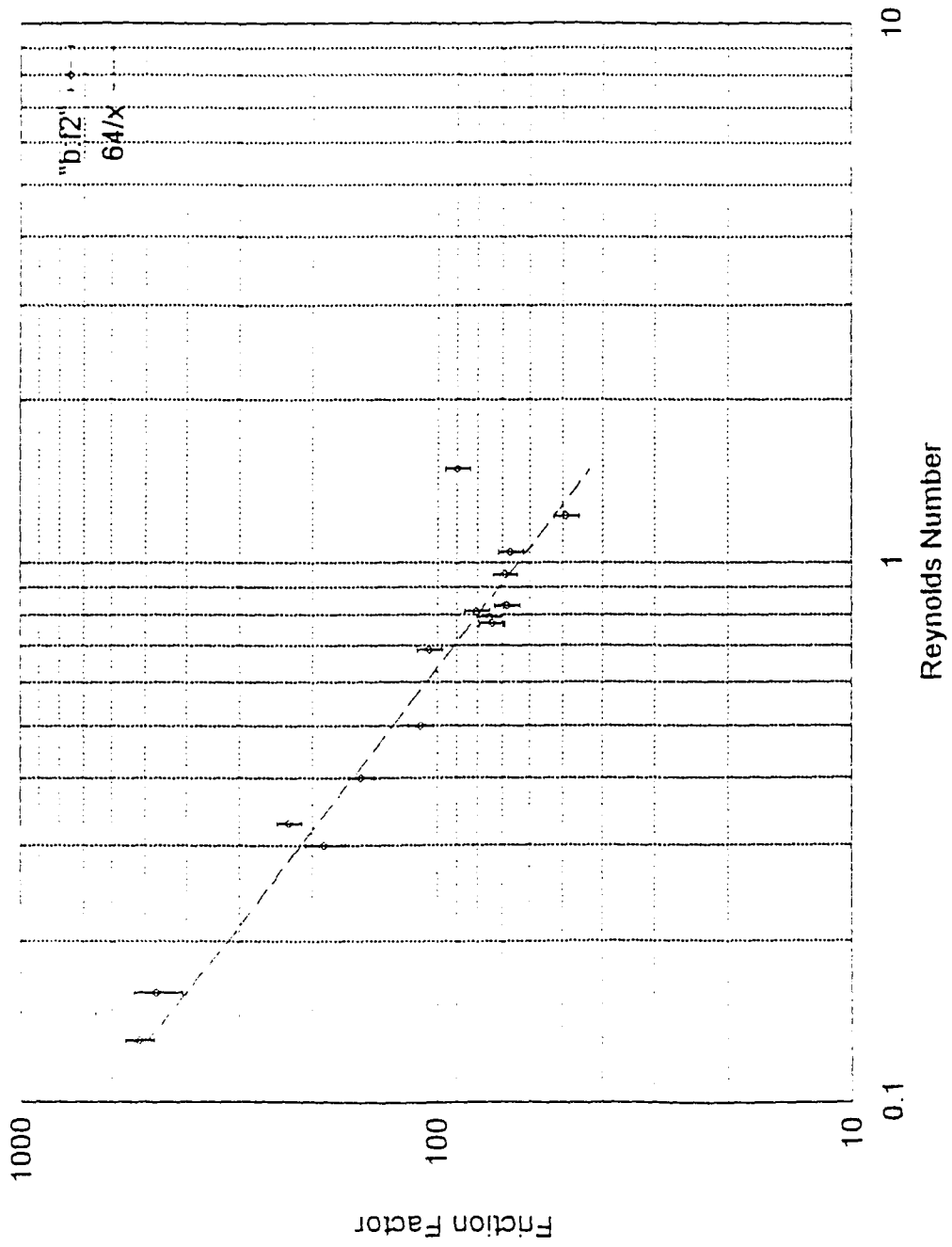


Figure 5.1 Friction Factor vs Reynolds Number for Straight Duct

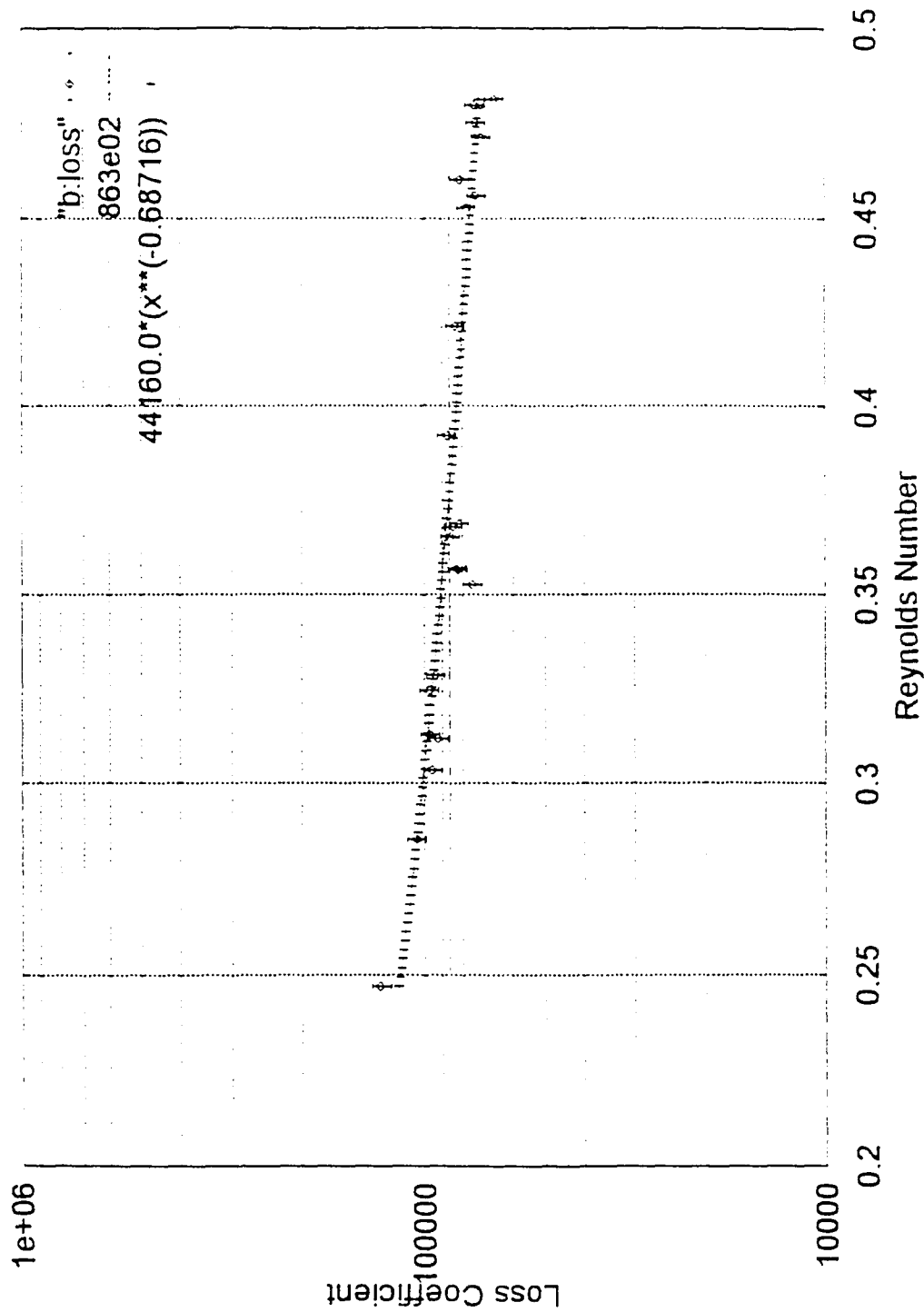


Figure 5.2 Loss Coefficient vs Reynolds Number for 20-Pore Perforation Plate

## Chapter 6

### Numerical Results

Modeling was done using NEKTON, a computational fluid dynamics package, to visualize the behavior of flow through the perforation plates.. This numerical work was used as a check for quick verification of the experimental data and was not intended to be comprehensive. NEKTON is a computer code for the simulation of steady and unsteady incompressible fluid flow and heat transfer, as well as optional convective-diffusive passive scalar quantities. NEKTON is based on the spectral element method; a high-order finite element technique for solving partial differential equations. The computational domain can be either stationary or moving. The package consists of three parts: PRENEK, NEKTON, and POSTNEK. It was used on a Silicon Graphics Iris workstation.

PRENEK is an interactive menu-driven program in which input conditions are specified for solving the problem. Density, average viscosity, inlet velocity distribution, diameter of the test section, length of the test section, and order of the polynomial were used as input parameters. The problem was solved as a two-dimensional steady flow problem for one flowrate.

NEKTON is the computational module that actually performs the numerical integration of the Navier-Stokes and energy equations. NEKTON uses standard quadrature formulas like Gaussian quadrature and Gauss-Lobatto quadrature to solve a polynomial.

POSTNEK is an interactive graphical package which displays and analyze the results of the NEKTON simulation. For the current study, NEKTON was used to

model the flow between two parallel plates and perforation plates were added. This simple Cartesian, 2-D model avoided the complexities involved with modeling the 3-D flow experienced through perforation plates. Velocity vectors, pressure profiles and the streamlines were visualized for the straight duct, 5-pore perforation plate, and 20-pore perforation plate in the POSTNEK session of the NEKTON simulation. For simple laminar flow between parallel plates, a Reynolds number of 0.66 was chosen to match the experimental runs in a circular pipe. The friction factor calculated from the Reynolds number of the numerical study for the straight duct was 97, which was very close to the experimental value of 90. The theoretical value predicted from  $f=64/Re$  was 43 .

Figure 6.1 shows the velocity vectors for the straight duct. Slow development of the flow from the inlet to outlet can be seen in the figure 6.1 due to an assumed uniform velocity distribution at the inlet. It took about four hydraulic diameters to attain a parabolic velocity profile consistent with laminar flow between two infinite sheets. The length of the test section corresponds to the distance along the x-axis and the diameter of test section corresponds the height along the y-axis. The length along the x-axis was 1830 mm and height along the y-axis was 38.1 mm. This problem was solved using 5th order polynomial and 256 elements with a grid size of 5.000e-02. The Reynolds number of the flow was 0.66 and the velocity of the flow was 1.50 mm/s.

Figure 6.2 shows the pressure profile obtained for a straight duct. The maximum pressure occurred at the inlet and minimum pressure at the outlet of the test section, respectively. The pressure drop was the difference between maximum and minimum pressures. The pressure drop computed for  $Re = 0.66$  was 40.15 Pa.

Figure 6.3 shows the streamlines for the straight duct. The figure showed that there was a disturbance in the streamlines due to the flow not being completely developed at the inlet of the test section. The streamlines become straight as soon as the flow developed fully.

Figure 6.4 shows the velocity vectors for the 5-pore perforation plate moving from the inlet towards the perforation plates and to the exit of the test section. The length along the x-axis was 1830 mm and height along y-axis was 38.1 mm. A parabolic profile was attained after the inlet section as the flow quickly developed into a fully-developed laminar flow. Maximum velocity obtained was 3.5 mm/s and the Reynolds number was 1.50. It took about 5 hydraulic diameters upstream and 2 hydraulic diameters downstream for the flow to become a fully developed parabolic profile.

Figure 6.5 shows the pressure contours for the 5-pore perforation plate. Pressure contours were not uniform at the inlet but they settled down gradually as the flow developed. The maximum pressure at the inlet was 122.5 Pa, minimum pressure at the outlet was -43.80 Pa, and the pressure drop was 166.3 Pa. The loss coefficient was 19,900.

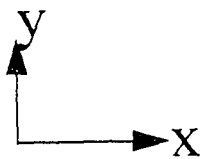
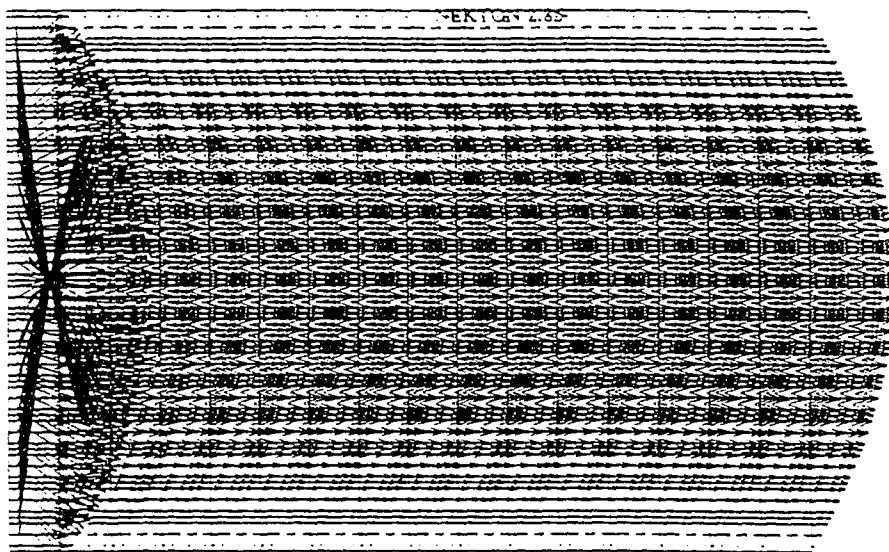
Figure 6.6 shows the streamlines for the 5-pore perforation plate. Streamlines were continuous, but there was a slight disturbance in the streamlines in the region between the inlet and the perforation plate. This problem could be avoided by dividing the larger elements present in this region into smaller elements and by increasing the order of the polynomial. Problem was solved using 5th order polynomial and 175 elements with a grid size of 5.000e-02.

Figure 6.7 shows the velocity vector plot for the 20-pore plate. Velocity vectors showed the development of a parabolic profile along the length of the test section. Velocity vectors were close together because the larger elements were divided into smaller elements along the length of the test section. The length along the x-axis was 1830 mm and height along the y-axis was 38.1 mm. Maximum velocity was 3.38 mm/s and the Reynolds number was 1.49. It took about 3 hydraulic diameters for the flow to become a fully developed parabolic profile.

Figure 6.8 shows the pressure profile for the 20-pore perforation plate. A gradual refinement of pressure contours between the elements near the inlet region

and the perforation plate can be seen in the figure. Maximum pressure at the inlet was 996 Pa and minimum pressure at the outlet was -181 Pa. The total pressure drop was 1177 Pa. The loss coefficient was 149.000.

Figure 6.9 shows the streamlines for the 20-pore perforation plate. Streamlines were continuous along the length, but there was a slight disturbance in the streamlines between the inlet region and the perforation plates. The reason for this disturbance could be the presence of the larger elements. Refinement can be achieved by dividing the larger elements into the smaller elements and by increasing the order of the polynomial. This problem was solved using 7th order polynomial and 420 elements with a grid size of  $7.000e-02$ . Comparison of the numerical and the experimental results is shown in the table 7.1.



x-length of the figure (1830 mm)  
y-height of the figure (38.1 mm)  
Reynolds number was (0.66)

**Figure 6.1 Plot of Velocity Vectors for a Straight Duct**

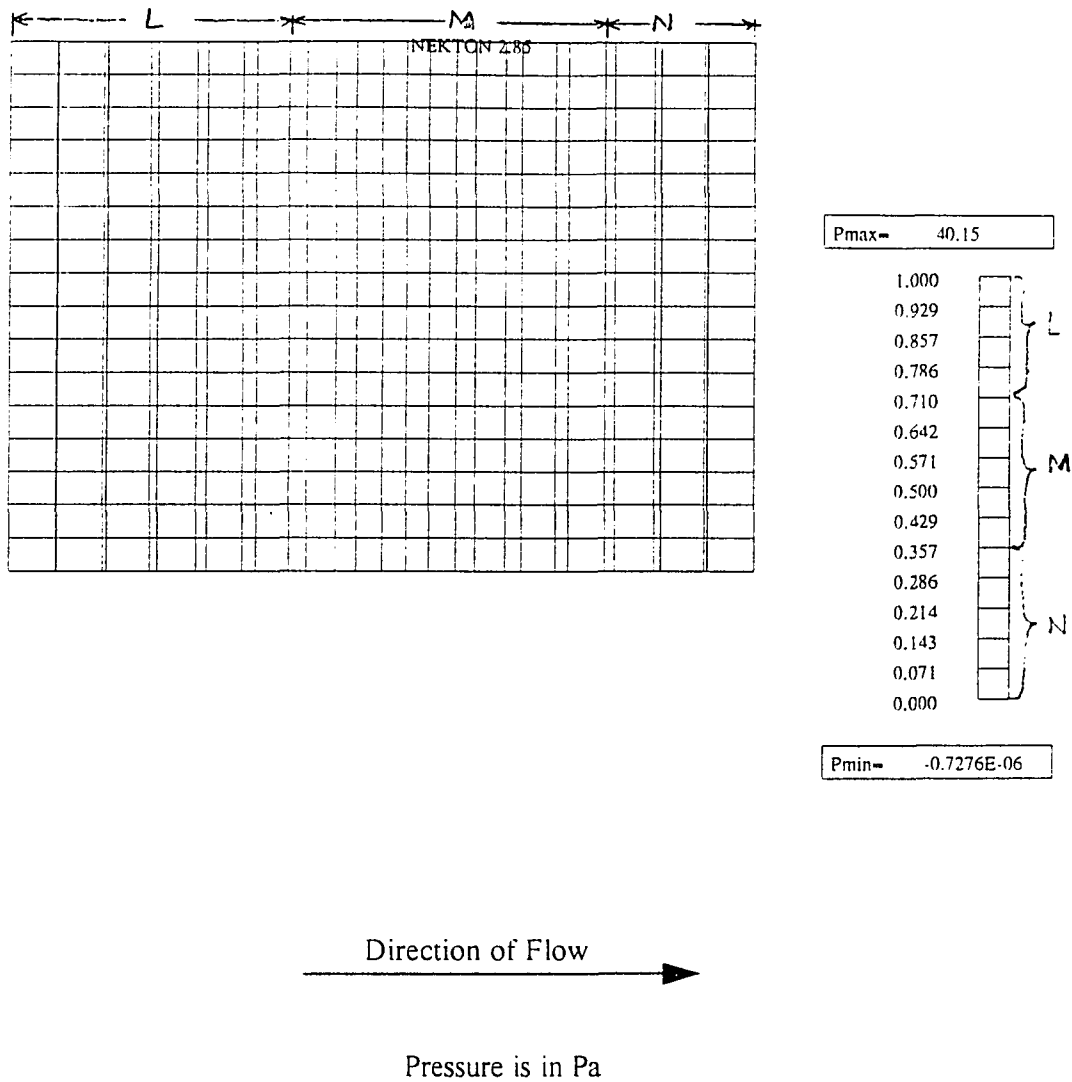


Figure 6.2 Plot of Pressure Profiles for a Straight Duct

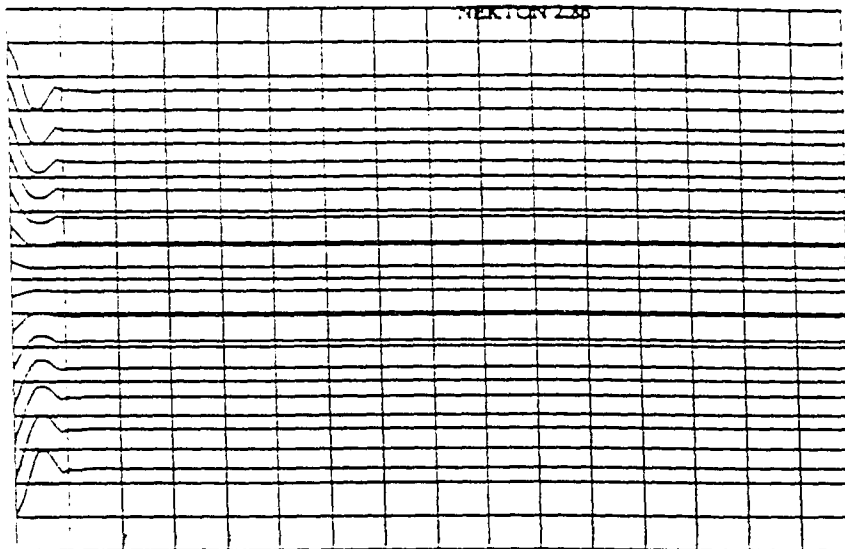
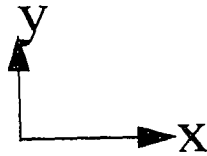
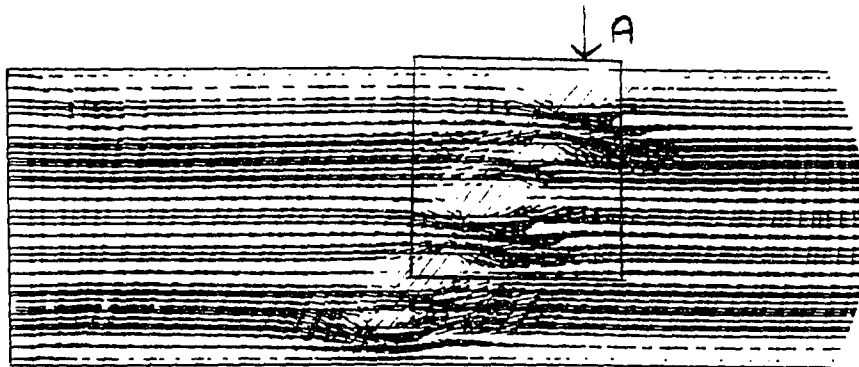
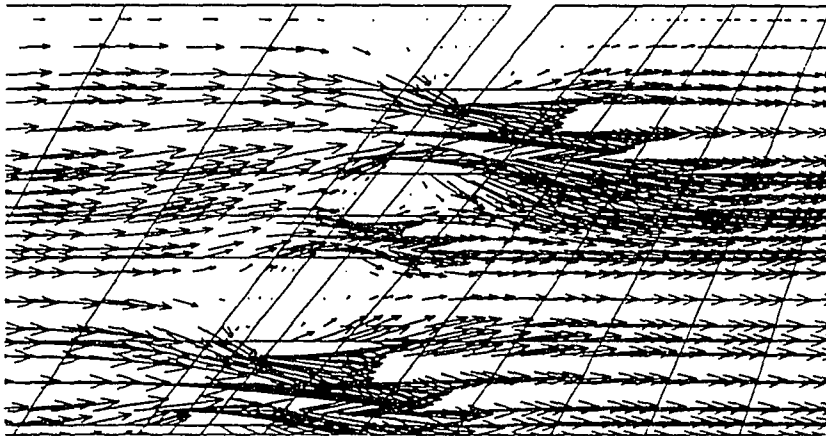


Figure 6.3 Plot of Streamlines for a Straight Duct

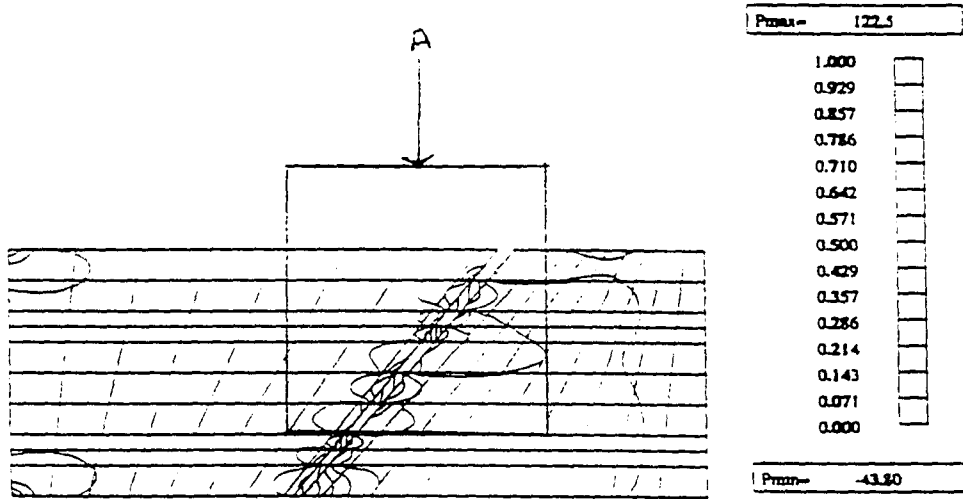


x-length of the figure (1830 mm)  
y-height of the figure (38.1mm)  
Reynolds number was (1.5)  
Loss Coefficient was 19900

**Figure 6.4 Plot of Velocity Vectors for the 5-Pore Perforation Plate**



**Figure 6.4.1** Velocity Vectors Emphasizing Portion A



Pressure Drop was 166 Pa

Figure 6.5 Plot of Pressure Profile for the 5-Pore Perforation Plate

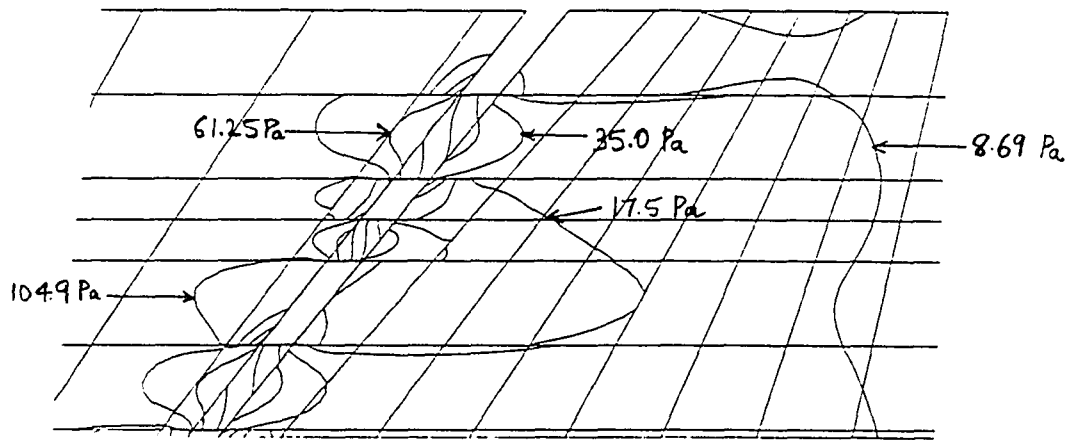
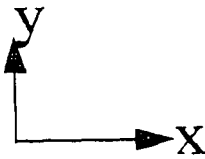
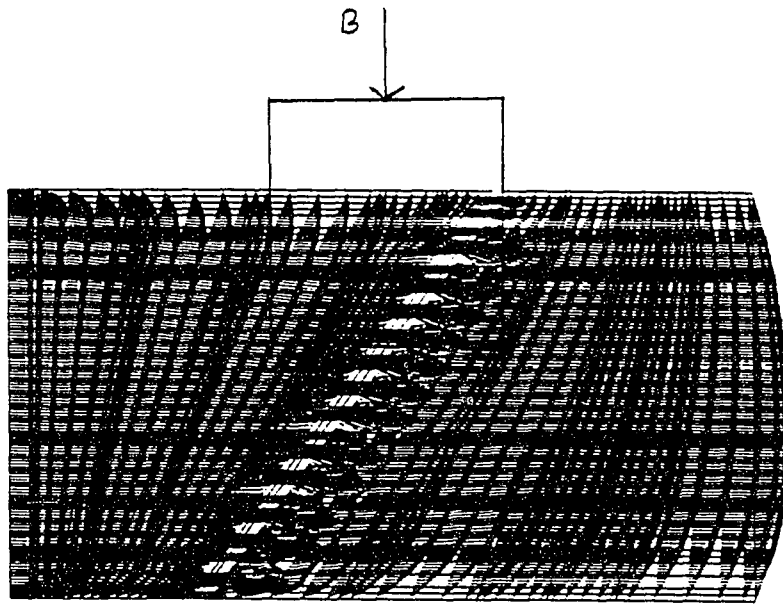


Figure 6.5.1 Pressure Profile Emphasizing Portion A



**Figure 6.6 Plot of Streamlines for the 5-Pore Perforation Plate**



x-length of the figure (1830 mm)  
y-height of the figure (38.1 mm)  
Reynolds number was (1.49)  
Loss coefficient was (149000)

**Figure 6.7 Plot of Velocity Vectors for the 20-Pore Perforation Plate**

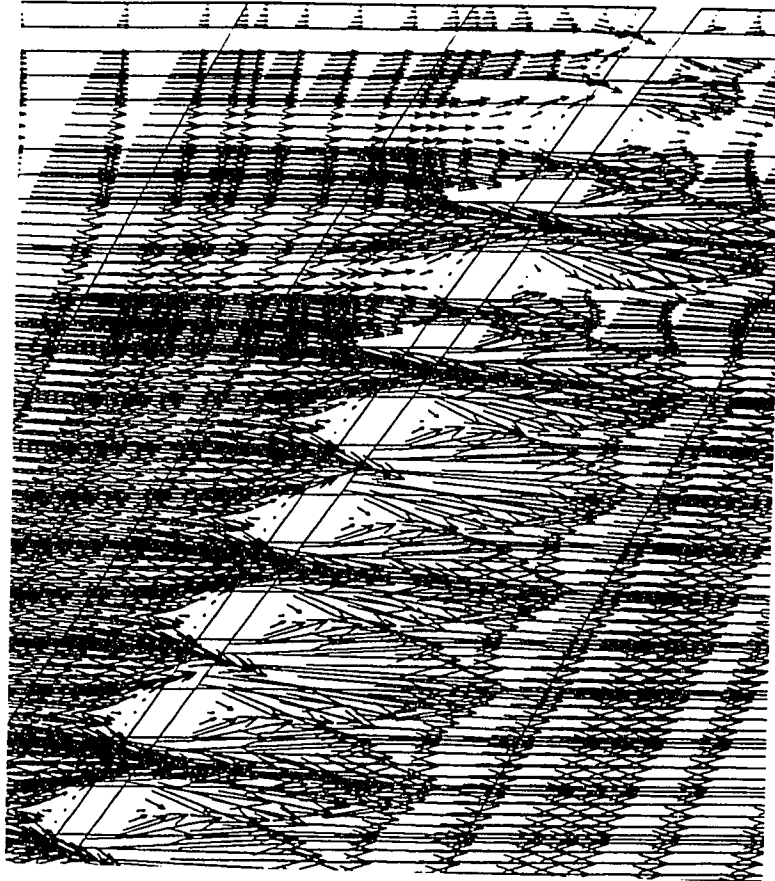


**Figure 6.7.1** Velocity Vectors Emphasizing Portion B

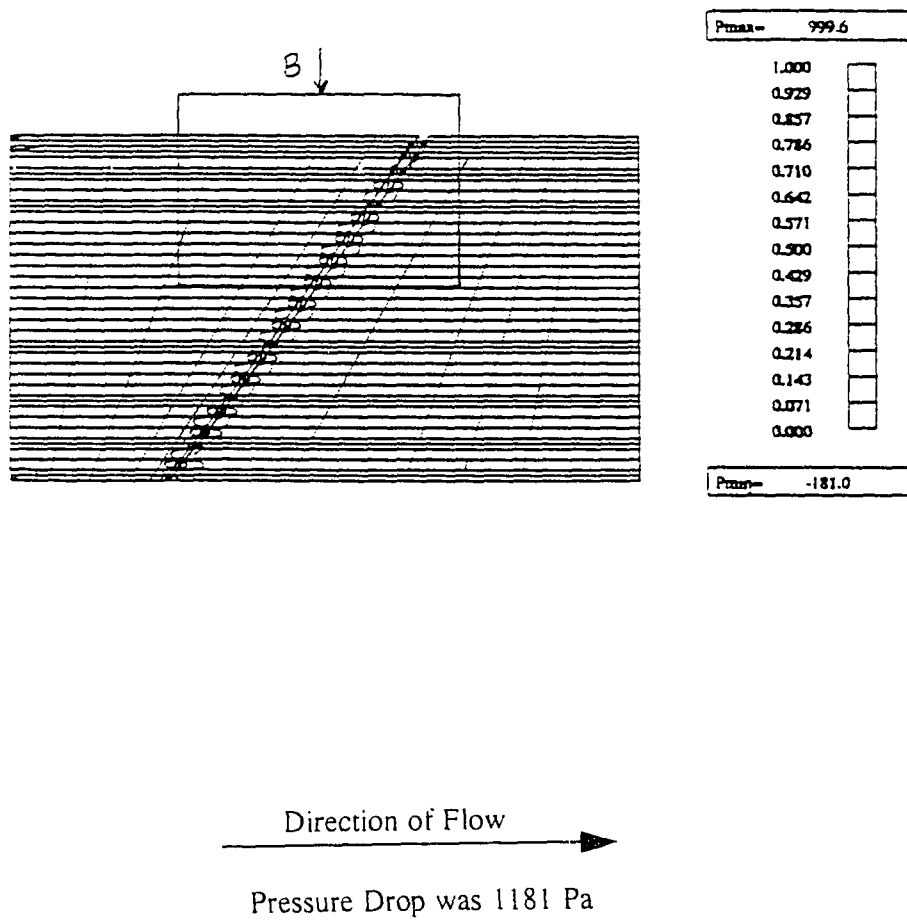
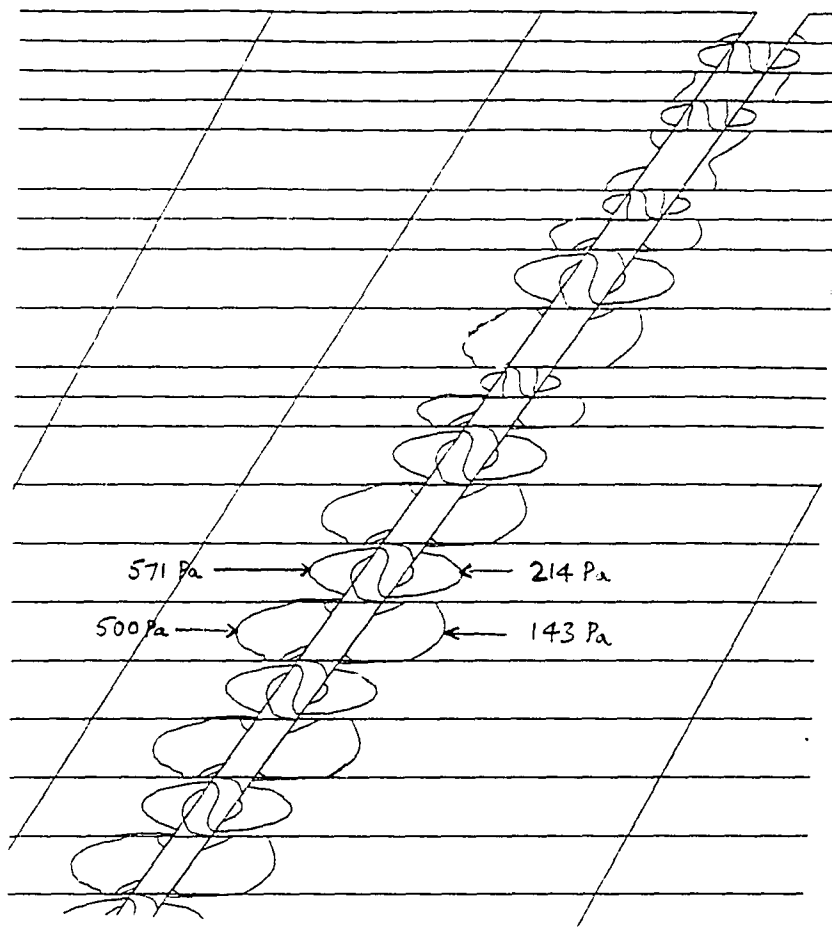
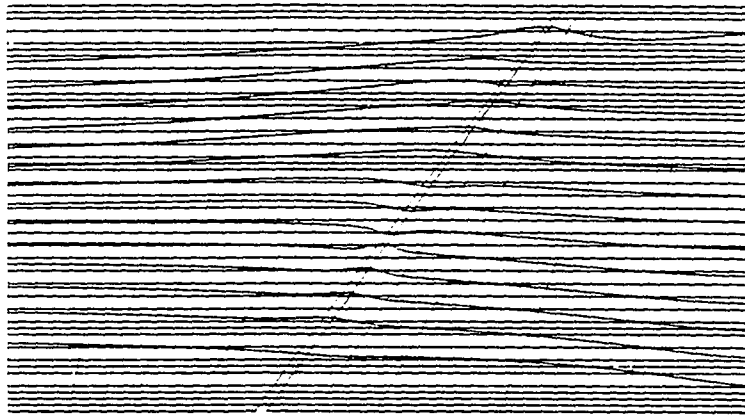


Figure 6.8 Plot of Pressure Profile for the 20-Pore Perforation Plate



**Figure 6.8.1 Pressure Profile Emphasizing Portion B**



**Figure 6.9 Plot of Streamlines for the 20-Pore Perforation Plate**

## Chapter 7

### CONCLUSIONS AND RECOMMENDATIONS

Behavior of the fluid flow through perforation plates present in the conducting vessels of plants was studied in this thesis. Pressures and velocities were measured by conducting three different experiments with a physical model of the plant cell. Corn syrup was used as the working fluid in all three experiments and some interesting observations were made. The role of the perforation plate is significant in obstructing the flow of fluid in the conducting vessels of the plants.

In the first experiment with a straight duct, there was a good agreement between the experimental and theoretical values of the friction factor. It was observed that corn syrup behaved as a Newtonian fluid.

In the second experiment, with a 5-pore perforation plate, the measured loss coefficient was very close to numerical values obtained from NEKTON simulation as shown in the table 7.1. The pressure drops measured were small and caused some problems in determining the loss coefficient. The average loss coefficient obtained from the experiment was 8947. In addition to the 5-pore perforation plate, another experiment was conducted with a 20-pore perforation plate which proved to be a better model of the actual plant xylem. Pressure drops measured with the 20-pore perforation plate were very high when compared to the values measured from the 5-pore perforation plate. In this experiment, it was observed that as the Reynolds number was increased there was a decrease in the loss coefficient. Loss coefficient values were very high because of the low velocities. The average loss coefficient obtained from the experiment was 86,300. Loss coefficient values were compared to the numerical

|                    | 5-Pore Perforation Plate |           | 20-Pore Perforation Plate |           |
|--------------------|--------------------------|-----------|---------------------------|-----------|
|                    | Experiment               | Numerical | Experiment                | Numerical |
| Pressure Drop (Pa) | 10                       | 166.3     | 51                        | 1177      |
| Velocity (m/s)     | 8.9e-04                  | 3.5e-03   | 7.5e-04                   | 3.383-03  |
| Reynolds Number    | 0.14                     | 1.5       | .25                       | 1.49      |
| Loss Coefficient   | 17,200                   | 19,900    | 130,000                   | 149,000   |

Table 7.1 Comparison of Experimental and Numerical Results

values obtained by NEKTON, and the values were in good agreement. The velocity vector plots obtained from the NEKTON showed the direction of the fluid flow in the xylem portion of the plant.

The 5-pore perforation plate had small effect on the overall resistance of the flow. Pressure drops measured were low because of the large spacing between the pores along the conducting vessels of the plants, and this did not have any impact on the resistance of the flow. The 20-pore perforation plate had more impact on the resistance of the flow because of small pore widths and high pressure drops. An increase in the pressure drop increased the overall hydraulic resistance and reduced the conducting capacity of the perforation plates.

The results of this work were expressed in terms of non-dimensional values: friction factor, loss coefficient, and Reynolds number. The advantage of using these non-dimensional values becomes apparent considering the fact that the same coefficients are applicable at identical Reynolds numbers regardless of the size of the plant xylem. Results also showed that as the number of pores in the perforation plate increased, pressure drop also increased across the plate.

There are many avenues for future research in this area. First, glycerin or motor oil of grade # 30 can be used as the working fluid in order to match the fluid flow. The chosen fluid must be transparent for flow visualization and must have a high viscosity to produce Reynolds numbers in the proper range. A change in the working fluid would be advisable since corn syrup dries out when exposed to air. This caused a change in the viscosity of the fluid and made it necessary to measure fluid viscosity for every run. Second, pressure sensors can be used in place of micromanometers to avoid problems due to air leakage within the micromanometer. Third, perforation plates with a greater number of pores can be tried at various angles in order to model the wide range of fluid flow observed in actual plants.

## APPENDIX I

### Computer Programs

#### A. Computer Program "Cor1"

This program was written in Microsoft Quickbasic to calculate the dynamic viscosity, Reynolds number, and friction factor for the fluid flow in the straight duct without any obstruction.

```
'*****
'
'   Program : cor1.bas
'   Purpose  : The purpose of the program is to calculate the dynamic viscosity, Reynolds
'               number, and the friction factor.
'   Date     : 01/31/95
'   Version  : 2
'   Author   : Anand Kanjerla
'*****
CLS
BEEP
'*****
'a1:    To Compute Flowrate
'*****
INPUT " 1. What is the volume of the fluid in the cylinder?(ml)  ", v
INPUT " 2. How much time does it take to fill the cylinder? (s)  ", t
volume = v / 1000000
q = volume / t
PRINT " flowrate(m^3/s):  "; q
'*****
'a2:    To Compute Velocity of the Fluid Flow in the Testsection.
'*****
d = 1.5 * .0254
```

```

Area = 3.14159265853# * (d / 2) ^ 2
PRINT " Area (m^2):      "; Area
velocity = q / Area
PRINT " velocity of the flow (m/s):      "; velocity
'*****
'a3:      To Compute Dynamic Viscosity of the Fluid.
'*****

Density.water = 1000
g = 9.81
Length.of.the.testsection = 1
INPUT " 3. What is the Manometer reading without flow? (mm) ", h0
INPUT " 4. What is the Manometer reading with the flow? (mm) ", h1
h0 = h0 / 1000
h1 = h1 / 1000
Delta.h.testsection = 2 * (h1 - h0)
Dynamic.Viscosity = Density.water * g * Delta.h.testsection * d ^ 2 / (32 *
                    Length.of.the.testsection * velocity)
PRINT " Dynamic.viscosity (kg/m-s):      "; Dynamic.Viscosity

'*****
'a4:      To Compute Reynolds Number of the Flow.
'*****

Density.corn syrup = 1394
Re = Density.corn syrup * velocity * d / Dynamic.Viscosity
PRINT " Reynolds number :      "; Re
'*****
'a5:      To Compute Theoretical Friction Factor.
'*****

f1 = 64 / Re
PRINT " Friction Factor:      "; f1

'*****
'a6:      To Compute Experimental Friction Factor.
'*****

f = Density.water * Delta.h.testsection * 2 * g * d / (Density.corn syrup * velocity ^ 2)
PRINT " Experimental Friction Factor:      "; f

END

```

## B. Computer Program "Cor2"

This program was written in Microsoft Quickbasic to calculate the dynamic viscosity of corn syrup for each experimental run based upon volumetric flowrate and measured pressure drops.

```

*****
'   Program: cor2.bas
'   Purpose : The purpose of the program is to calculate the Dynamic Viscosity of the Corn
               Syrup.
'   Date    : 01/31/95
'   Version : 1
'   Author  : Anand Kanjerla
*****

CLS
BEEP

*****
' h1:   To Calculate Deltah of the Testsection
*****
INPUT "1. What is the manometer reference reading? (mm) ", h0
INPUT "2. What is the manometer reading with flow? (mm) ", h1
h0 = h0 / 1000!
    h1 = h1 / 1000!
    delta.h = 2 * (h1 - h0)

*****
' h2:   To Calculate Velocity of Fluid flow in the testsection
*****
INPUT "3. What is the volume of fluid in the graduated cylinder? (ml) ", V
INPUT "4. How long did it take to fill the graduated cylinder? (s) ", t
V = V / 1000000!
Volumetric.flowrate = V / t
area = 3.14159265853# * (.75 * .0254 / 2) ^ 2
Velocity = Volumetric.flowrate / area

```

```

*****
' b3:   To Calculate Dynamic Viscosity of the Fluid in Testsection
*****

g = 9.81
density.water = 1000
L = 1!
d = .75 * .0254
Dynamic.viscosity = density.water * g * delta.h * d ^ 2 / (32 * L * Velocity)
PRINT
PRINT "OUTPUT"
PRINT "1. Volumetric flowrate (m^3/s):      ";    volumetric.flowrate
PRINT "2. Cross sectional area (m^2):      ";    area
PRINT "3. Velocity (m/s):                  ";    velocity
PRINT "4. Dynamic viscosity (kg/m-s):      ";    Dynamic.viscosity
END

```

### C. Computer Program "Cor3"

This program was written in Microsoft Quickbasic. The purpose of this program is to calculate the uncertainty in the dynamic viscosity of corn syrup.

```

*****
'   Program : cor3.bas
'   Purpose  : The purpose of the program is to calculate the uncertainty in the Dynamic
                Viscosity.
'   Date    : 01/31/94
'   Version  : 2
'   Author   : Anand Kanjerla
*****

CLS
BEEP

```

```

*****
' C1:   To Compute the Uncertainty in Flowrate
*****
INPUT " 1. What is the uncertainty in the volume? (ml)      ",      u.volume
INPUT " 2. What is the volume of the fluid in the cylinder? (ml) ",      volume
INPUT " 3. What is the uncertainty in the time? (s)         ",      u.time
INPUT " 4. How long did it take to fill the cylinder? (s)   ",      total.time

Flowrate = volume * .000001 / total.time
PRINT " Flowrate : (m^3/s)      ": Flowrate
u.Flowrate = Flowrate * SQR((u.volume / volume) ^ 2 + (u.time / total.time) ^ 2)
PRINT "   Uncertainty in Flowrate (m^3/s):  ": u.flowrate
*****

' C2:   To Compute the Uncertainty in the Area of Smalltube
*****
INPUT " 5. What is the Uncertainty in diameter of the Smalltube? (m) ", u.diameter.smalltube
INPUT " 6. What is the diameter of the Smalltube? (m)           ", diameter.smalltube

Area.smalltube = 3.1415926# * (diameter.smalltube / 2) ^ 2
PRINT " Area.smalltube: (m^2) ": Area.smalltube

u.Area.smalltube = Area.smalltube * SQR((u.diameter.smalltube /
diameter.smalltube) ^ 2)

PRINT "   Uncertainty in the Area of the Smalltube: (m^2) ": u.Area.smalltube

*****

' C3:   To Compute the Uncertainty in the Velocity of Smalltube
*****

Velocity.smalltube = Flowrate / Area.smalltube
PRINT " Velocity.smalltube: (m/s) ": Velocity.smalltube

u.Velocity.smalltube = Velocity.smalltube * SQR((u.Flowrate / Flowrate) ^ 2
+(u.Area.smalltube / Area.smalltube) ^ 2)

PRINT "Uncertainty in the Velocity in the Smalltube: (m/s) ": u.Velocity.smalltube

```

```

'*****'
' C4:    To Compute the Uncertainty in the Viscosity of Fluid
'*****
INPUT " 6. What is the Uncertainty in the Length of the Smalltube?(m) ", u.Length.smalltube
INPUT " 7. What is the Length of the smalltube? (m)", Length.smalltube
INPUT " 8. What is the Uncertainty in Delta h of the Smalltube? (m) ", u.Deltah.smalltube
INPUT " 9. What is the Delta h of the Smalltube? (m) ", Deltah.smalltube

density.water = 1000!
g = 9.81

Viscosity = density.water * g * Deltah.smalltube * diameter.smalltube ^ 2 / (32! *
Length.smalltube * Velocity.smalltube)

PRINT " viscosity: (kg/m-s)"; viscosity

u.Viscosity = Viscosity * SQR((2 * u.diameter.smalltube / diameter.smalltube) ^ 2 +
(u.Length.smalltube / Length.smalltube) ^ 2 + (u.Velocity.smalltube /
Velocity.smalltube) ^ 2 + (u.Deltah.smalltube / Deltah.smalltube) ^ 2)

PRINT " Uncertainty in the Viscosity of the Fluid: (kg/m-s) "; u.Viscosity

END

```

#### D. Computer program "Cor4"

This program was written in Microsoft Quickbasic to calculate the Reynolds number, pressure drop, and loss coefficient in the 5 pore and 20 pore perforation plate.

```

*****
' Program : cor4.bas
' Purpose : The purpose of the program is to calculate the Reynolds number, pressure drop and
the loss coefficient in the 5 pore and 20 pore perforation plate.
' Date : 01/31/95
' Version : 2
' Author : Anand Kanjerla
'*****

CLS
BEEP

```

```

*****
' D1: To Compute Deltah of the Testsection
*****
INPUT " 1. What is the manometer reference reading of test section? (mm) ", h0
INPUT " 2. What is the manometer reading with flow of test section? (mm) ", h1
    h0 = h0 / 1000
    h1 = h1 / 1000
    delta.h.testsection = 2! * (h1 - h0)
*****
' D2: To Compute Dynamic Viscosity of the Fluid
*****
INPUT " 3. What is the volume of fluid in the graduated cylinder? (ml) ", v
    volume = v / 1000000! ' convert the volume to m^3.
INPUT " 4. How long did it take to fill the graduated cylinder? (s) ", time.to.fill
    volumetric.flowrate = volume / time.to.fill
    d.testsection = 1.5 * .0254
    area.testsection = 3.14159265853# * (d.testsection / 2!) ^ 2
    velocity.testsection = volumetric.flowrate / area.testsection
    g = 9.81
    density.water = 1000!
    density.corn.syrup = 1394!
    length.of.testsection = 1!
    dynamic.viscosity = XXXXXX
*****
' D3: To Compute Re in the Testsection
*****
Re.testsection = density.corn.syrup * velocity.testsection * d.testsection / dynamic.viscosity
*****
' D4: To Compute the Pressure Drop in Testsection due to Obstruction and
the Smooth wall, combined.
*****
pressure.of.obs.plus.smooth.wall = density.water * g * delta.h.testsection
*****
' D5: To Calculate the Pressure Drop in Testsection due to Smooth wall of the pipe alone.
*****
friction.factor = 64 / Re.testsection
hf = friction.factor * length.of.testsection * velocity.testsection ^ 2 / (2! * g *
    d.testsection)
pressure.of.smooth.wall = density.corn.syrup * g * hf

```

```

*****
' D6:   To Calculate the Pressure Drop in Testsection due to Obstruction, alone.
' *****
pressure.of.obs = pressure.of.obs.plus.smooth.wall - pressure.of.smooth.wall

*****
' D7:   Compute the loss coefficient.
' *****
loss.coefficient = 2! * pressure.of.obs / (density.corn.syrup * velocity.testsection ^ 2)

' *****
' D8:   PRINTOUT OF RESULTS.
' *****
CLS
PRINT
PRINT "OUTPUT"
PRINT " "
PRINT "  A. Viscosity Measurement Tube Information:"
PRINT "  1. Volumetric flowrate (m^3/s):      "; volumetric.flowrate
PRINT "  2. Dynamic viscosity (kg/m-s):      "; dynamic.viscosity
PRINT "  B. Pressure Drop Data in Test Seection."
PRINT "  1. Reynolds number in the testsection: "; Re.testsection
PRINT "  2. Velocity (m/s):                    "; velocity.testsection
PRINT "  3. Area testsection (m^2):            "; area.testsection
PRINT "  4. Friction factor:                   "; friction.factor
PRINT "  5. Head loss in the testsection (m):   "; hf
PRINT "  6. Pressure Drop (obs. + wall) (Pa):  "; pressure.of.obs.plus.smooth.wall
PRINT "  7. Pressure Drop (wall alone) (Pa):   "; pressure.of.smooth.wall
PRINT "  8. Pressure Drop (obstruction) (Pa):  "; pressure.of.obs
PRINT "  9. Loss coefficient, K:               "; loss.coefficient

END

```

### E. Computer Program "Cor5"

The purpose of this program is to calculate the uncertainties in the Reynolds number, pressure drop, and loss coefficient in 5-pore and 20-pore perforation plates.

```

*****
'   Program : cor5.bas
'   Purpose : The purpose of the program is to calculate the uncertainties in the reynolds
              number, pressure drop and loss coefficient of a 5 pore and a 20 pore perforation
              plate.
'   Date    : 01/31/95
'   Version : 2
'   Author  : Anand Kanjerla
*****
CLS
BEEP
*****
'   E1. To Compute the Uncertainty in Flowrate
*****
      BEEP
      INPUT " 1. What is the volume of the fluid in the cylinder? (ml) ", volume
      BEEP
      INPUT "   a. What is the uncertainty in the volume? (ml) ",          U.volume
      BEEP
      INPUT " 2. How long did it take to fill the cylinder? (s) ",          total.time
      BEEP
      INPUT "   a. What is the uncertainty in the time? (s) ",          U.total.time
              flowrate = volume * .000001 / total.time
              Uq = flowrate * SQR((U.volume / volume) ^ 2 + (U. total.time / total.time) ^ 2)
      PRINT " > Uncertainty in Flowrate (m^3/s): "; Uq
*****
'   E2. To Compute the Uncertainty in Area of Testsection
*****
      BEEP
      INPUT " 3. What is the Diameter of the testsection? (m) ",          dt
      BEEP
      INPUT " 4. What is the Uncertainty in Diameter of the testsection? (m) ",          Udt
              area.testsection = 3.1415926# * dt ^ 2 / 4!
              Ua = area.testsection * SQR((Udt / dt) ^ 2)
      PRINT " > Uncertainty in the Area of the testsection: (m^2) "; Ua
*****
'   E3. To Compute the Uncertainty in the Velocity of Testsection
*****
              vt = flowrate / (area.testsection)
              Uvt = vt * SQR((Uq / flowrate) ^ 2 + (Ua / area.testsection) ^ 2)

```

```

PRINT " > Uncertainty in the Velocity in the testsection: (m/s) "; Uvt
'*****
' E4. To Compute the Uncertainty in Reynolds number of the Testsection
'*****
    BEEP
INPUT " 4. What is the Viscosity of the corn syrup (kg/m-s)? ", vis
    BEEP
INPUT " a. Uncertainty, (kg/m-s)? ", Uvis
    BEEP
INPUT " 5. What is the Density of the Corn Syrup (kg/m^3)? ", den
    BEEP
INPUT " a. Uncertainty, (kg/m^3)? ", Uden
    BEEP
INPUT " 6. What is the Reynolds number of testsection? ", ret
    Uret = ret * SQR((Uden / den) ^ 2 + (Uvt / vt) ^ 2 + (Udt / dt) ^ 2 + (Uvis / vis) ^ 2)
PRINT " > Uncertainty in Reynolds number of testsection: ", Uret
'*****
' E5. To Compute the Uncertainty in the Pressure Drop of the smooth plus Obstruction wall.
'*****
    BEEP
INPUT " 7. What is the Delta h of the Testsection (m of water)? ", h1
    BEEP
INPUT " a. Uncertainty, (m of water)? ", Uh1
    BEEP
INPUT " 8. What is the Pressure Drop of Smooth plus Obstruction wall (pa)? ", p1
    Up1 = p1 * SQR((Uh1 / h1) ^ 2)
PRINT " > Uncertainty, (pa): "; Up1

'*****
' E6. To Compute the Uncertainty in the Pressure Drop of Smooth Wall
'*****
    BEEP
INPUT " 24. What is the Friction Factor in the Testsection? ", f
    Uf = f * SQR((Uret / ret) ^ 2)
PRINT " uncertainty.in.the.Friction Factor: "; Uf
    BEEP
INPUT " 27.What is the Uncertainty.in.the.Length.of.Testsection? ", Ult
    BEEP
INPUT " 28.What is the Length.of.Testsection? ", Lt
    BEEP
INPUT " 29.What is the Headloss.in.the.Testsection? ", hf
    Uhf = hf * SQR((Uf / f) ^ 2 + (Ult / Lt) ^ 2 + (2 * Uvt / vt) ^ 2 + (Udt / dt) ^ 2)

```

```

PRINT " > Uncertainty in Headloss of Testsection:(m) "; Uhf
BEEP
INPUT " 30.What is the Pressure.Drop.of.Smoothwall? ", p0
Up0 = p0 * SQR((Uden / den) ^ 2 + (Uhf / hf) ^ 2)
PRINT " > Uncertainty (mm of water) "; Up0
'*****
' E7. To Compute the Uncertainty in the Loss Coefficient.
'*****
IF Up1 > Up0 THEN Up = Up1 ELSE Up = Up0
INPUT " 31.What is the uncertainty in the pressure.drop.of.obstruction.alone ? "; Up
BEEP
INPUT " 32.What is the Pressure.Drop.of.obstruction.alone? ", p
BEEP
INPUT " 33.What is the Loss.Coefficient? ", K
Uk = K * SQR((Up / p) ^ 2 + (Uden / den) ^ 2 + (-2 * Uvt / vt) ^ 2)
PRINT " > Uncertainty in Loss.coefficeint: "; Uk

END

```

## APPENDIX II

### Tabulated Results

| Reynolds Number | Experimental Friction Factor | Uncertainty in Friction Factor |
|-----------------|------------------------------|--------------------------------|
| 0.13            | 516                          | 39                             |
| 0.16            | 471                          | 60                             |
| 0.3             | 187                          | 21                             |
| 0.33            | 228                          | 16                             |
| 0.4             | 153                          | 11                             |
| 0.5             | 110                          | 8                              |
| 0.69            | 105                          | 7                              |
| 0.77            | 74                           | 5                              |
| 0.79            | 75                           | 5                              |
| 0.81            | 81                           | 6                              |
| 0.83            | 68                           | 4.8                            |
| 0.95            | 69                           | 4.8                            |
| 1.05            | 67                           | 4.7                            |
| 1.22            | 49                           | 3.5                            |
| 1.49            | 90                           | 6.3                            |

Table II.1 Data for the Plot of Friction Factor vs Reynolds Number for the Straight Duct

| Reynolds Number | Loss Coefficient | Uncertainty in Loss Coefficient |
|-----------------|------------------|---------------------------------|
| 8.55e-2         | 28109            | 475                             |
| 1.37e-1         | 17215            | 127                             |
| 1.78e-1         | 12511            | 683                             |
| 1.78e-1         | 13739            | 122                             |
| 1.84e-1         | 13496            | 423                             |
| 1.89e-1         | 9829             | 582                             |
| 1.97e-1         | 3589             | 50                              |
| 2.08e-1         | 5027             | 1440                            |
| 2.11e-1         | 6192             | 58                              |
| 2.31e-1         | 10976            | 2979                            |
| 2.40e-1         | 2831             | 1128                            |
| 2.41e-1         | 4810             | 3497                            |
| 2.42e-1         | 2133             | 2132                            |
| 2.44e-1         | 4772             | 3090                            |
| 2.65e-1         | 6124             | 1445                            |
| 3.21e-1         | 1807             | 1141                            |

Table II.2 Data for 5-Pore Perforation Plate

Data reported in table II.2 is questionable. As the pressure drop measured was low, it caused large variations in the loss coefficient values. Therefore this data may not be used as reference for future work.

| Reynolds number | loss coefficient | uncertainty in loss coefficient |
|-----------------|------------------|---------------------------------|
| 0.2470          | 128216           | 6867                            |
| 0.2854          | 104520           | 5582                            |
| 0.3035          | 95569            | 5077                            |
| 0.3119          | 92226            | 4908                            |
| 0.3127          | 96982            | 5145                            |
| 0.3244          | 97187            | 5167                            |
| 0.3284          | 93667            | 4972                            |
| 0.3524          | 75696            | 4033                            |
| 0.3565          | 82143            | 4364                            |
| 0.3569          | 82987            | 4407                            |
| 0.3652          | 86029            | 4560                            |
| 0.3679          | 84481            | 4482                            |
| 0.3687          | 81558            | 4382                            |
| 0.3921          | 87569            | 4668                            |
| 0.4214          | 83479            | 4441                            |
| 0.4526          | 78161            | 4139                            |
| 0.4558          | 73999            | 3921                            |
| 0.4602          | 81115            | 4289                            |
| 0.4714          | 71912            | 3810                            |
| 0.4755          | 74218            | 3926                            |
| 0.4799          | 74859            | 3961                            |
| 0.4815          | 66521            | 3534                            |

Table II.3 Data for the Plot of Loss Coefficient vs Reynolds Number for 20-Pore Perforation Plate

## References

- Dodge, A.R, and Thompson, J.M., **Fluid Mechanics**, McGraw-Hill Book Company, Inc., 1937.
- Giordano. R., Salleo. A., Salleo. S., and Wanderlingh. F, "Flow in Xylem Vessels and Poiseuille's Law," *Canadian Journal of Botany*, 56(5) , 333-338, 1977.
- Holman. J. P, **Experimental Methods for Engineers**, McGraw-Hill Book Company, Inc., 1978.
- Liggett, A.J., **Fluid Mechanics**, McGraw-Hill Book Company, Inc.,1994.
- Milburn, A.J., **Water Flow in Plants**, Longman Group Limited, 1979.
- Nekton**, Version 2.85, Nektonics Inc, 1992.
- Pickard, W. F., "The Ascent of Sap in Plants," *Progress in Biophysics and Molecular Biology*, 37, 181-229, 1981.
- Sutcliffe. J., **Plants and Water**, Edward Arnold Publishers Limited,1968.
- Schulte, P. J., Arthur, C.G, Park, S. N, "Water Flow in Vessels With Simple Compound Perforation Plates," *Annals of Botany* (64), 171-178,1989.
- Schulte, P. J., Arthur, L.C, "Water Flow Through Vessel Perforation Plates - A Fluid Mechanical Approach," *Journal of Experimental Botany*, 44(7), 1135-1142, 1993.
- Schulte, P. J., Arthur, L.C, " Water Flow Through Vessel Perforation Plates - The Effects of Plate Angle and Thickness for *Liriodendron tulipifera*," *Journal of Experimental Botany*, 44(7), 1143-1148, 1993.
- Viswanath, D. S., and Natarajan G., **Data Book on the Viscosity of Liquids**, Hemisphere Publishing Corporation, 1984.

Zimmermann, M. H., **Xylem Structure and the Ascent of Sap**, Springer-Verlag  
Berlin Heidelberg New York, 1983.

White, M. F., **Viscous Fluid Flow**, McGraw-Hill , Inc., 1991.